NASA Contractor Report 181698

ICASE REPORT NO. 88-46

ICASE

NONLINEAR TOLLMIEN-SCHLICHTING/VORTEX

INTERACTION IN BOUNDARY LAYERS

P. Hall

F. T. Smith

Contract No. NAS1-18107
August 1988

INSTITUTE FOR COMPUTER APPLICATIONS IN SCIENCE AND ENGINEERING
NASA Langley Research Center, Hampton, Virginia 23665

Operated by the Universities Space Research Association

National Aeronautics and
Space Administration

Langley Research Center
Hampton, Virginia 23665

NONLINEAR TOLLMIEN-SCHLICHTING/VORTEX INTERACTION IN BOUNDARY LAYERS

P. Hall
Department of Mathematics
Exeter University
Exeter, EX4 4QE, U.K.

F. T. Smith
Department of Mathematics
University College London
Gower Street
London, WC1E 6BT, U.K.

ABSTRACT

The nonlinear interaction between two oblique three-dimensional Tollmien-Schlichting (TS) waves and their induced streamwise-vortex flow is considered theoretically for an incompressible boundary layer. The same theory applies to the de-stabilization of an incident vortex motion by sub-harmonic TS waves, followed by interaction. The scales and flow structure involved are addressed for high Reynolds numbers. The nonlinear interaction is powerful, starting at quite low amplitudes with a triple-deck structure for the TS waves but a large-scale structure for the induced vortex, after which strong nonlinear amplification occurs. This includes nonparallel-flow effects. The nonlinear interaction is governed by a partial-differential system for the vortex flow coupled with an ordinary-differential one for the TS pressure. The solution properties found sometimes produce a break-up within a finite distance and sometimes further downstream, depending on the input amplitudes upstream and on the wave angles, and that then leads on to the second stages of interaction associated with higher amplitudes, the main second stages giving either long-scale phenomena significantly affected by nonparallelism or shorter quasi-parallel ones governed by the full nonlinear triple-deck response. Qualitative comparisons with experiments are noted.

This research was supported by the National Aeronautics and Space Administration under NASA Contract No. NAS1-18107 while the authors were in residence at the Institute for Computer Applications in Science and Engineering (ICASE), NASA Langley Research Center, Hampton, VA 23665.

1. INTRODUCTION

The idea of significant interactions arising between oblique Tollmien-Schlichting (TS) waves and induced, or incident, streamwise vortices has been circulating for some considerable time, as a possible or even a probable early stage in transition to turbulence in boundary layers and duct flows. In the boundary-layer context there is some experimental evidence of such interactions occurring in practice (Aihara et al., 1965, 1969, 1981, 1985; Tani and Sakagami, 1962; Bippes and Görtler, 1972; and possibly Klebanoff, Tidstrom and Sargent, 1962), as well as supporting computational work (see Wray and Hussaini, 1984 and Spalart and Yang, 1986, the latter showing the emergence of oblique waves from random initial disturbances), for flat or curved surfaces. The theoretical idea is basically this in principle: if two low-amplitude TS waves represented by $(\alpha_1, \pm\beta_1, \Omega_1)$ are present, i.e. each with a streamwise wavenumber α_1 and a frequency Ω_1, but with opposite spanwise wavenumbers $\pm\beta_1$, then nonlinear inertial effects produce the combination $(\alpha_1 - \alpha_1, \beta_1 + \beta_1, \Omega_1 - \Omega_1)$ at second order, among other contributions, i.e., the standing wave or streamwise vortex flow $(0, 2\beta_1, 0)$ is induced. Equally, the combination of the vortex $(0, 2\beta_1, 0)$ and one TS wave $(\alpha_1, \beta_1, \Omega_1)$ provokes the other TS wave $(\alpha_1, -\beta_1, \Omega_1)$ also. So nonlinear interaction takes place between the three-dimensional (3D) TS waves and the vortex. Such interplay may start from a single 3D TS wave dominating at first, upstream, with a minor amount of the other TS wave and hence of the induced vortex, or it may be initiated by an incident vortex upstream, with the TS waves then developing at first as small disturbances of the boundary-layer-plus-vortex motion. Both situations are observed experimentally or computationally. In either situation the ensuing nonlinear interaction downstream may be expected to have the same character to some extent, although possibly with considerably different end results, depending on the input conditions upstream. There is a possible connection here in fact with the use of vortex generators in laminar-flow control (Bushnell, 1984) in boundary layers.

Little progress has been made, however, in actually converting the above notion into nonlinear TS/vortex interaction equations in a rational theoretical way consistent with the Navier-Stokes equations. The only such theoretical study appears to be that of Hall and Smith (1987, see also references therein), but that applies to channel-flow interactions. A major difficulty exists in moving on to the boundary-layer context, namely to make allowance consistently for the growth or decay of the basic steady boundary layer, say on an airfoil, i.e. to incorporate nonparallel-flow effects. These effects are known to be substantial in Görtler-vortex development on a curved surface (Hall, 1982, 1988 and references therein) and in TS waves to some extent (Smith, 1979a and references therein), and likewise they are potentially significant in the long TS-induced vortices or incident vortices of

present concern for a flat or curved surface. A second major task is to pin down the main scales, and hence the flow structure, involved in a TS/vortex interaction in a boundary layer, and the scales are also affected by the nonparallelism present. Our aim here is to incorporate these two aspects in a self-consistent theory to begin tackling boundary-layer TS/vortex interaction. Mention should be made at this stage of the theoretical approximations by Benney and Lin (1960), Antar and Collins (1975), Srivastava and Dallmann (1987), among others, all of which are of undoubted interest in their attempts to address various levels of weak interaction, but all of which are in the end inconsistent with the Navier-Stokes equations. This is due much to the nonparallel-flow effects acting at finite Reynolds numbers: see also later comments.

The current approach takes advantage of the feature that the Reynolds numbers (Re) of interest in reality are very large. So Re is taken as a large parameter throughout. Previous discussions (e.g., Smith, 1979a,b; Hall, 1982; Hall and Smith, 1984; Ryzhov and Zhuk, 1986; Smith and Stewart, 1987) show that the large-Re approach is in fact the only way to obtain a consistent theory for boundary-layer instabilities and transition, apart from large-scale computations of the 3D unsteady Navier-Stokes equations of course, and thus, in a sense, there in no competing theory as far as we are aware. Further, as a bonus, the comparisons with experiments and computations presented in the above papers, when combined with the numerical interpretations of Smith, Papageorgiou and Elliott (1984), tend to verify the practical value of the current type of approach at the Reynolds numbers of real concern.

The scales and the flow structure involved in the TS/induced-vortex interaction in an incompressible boundary layer are examined in sections 2-4 below. They are based only loosely on our channel-flow study (1987) and have to accommodate the shortness of the triple-deck streamwise length scale in the typical 3DTS wave compared with the longer scale of the typical vortex affected by nonparallelism (Smith, 1979a,b; Hall and Smith, 1984). Whether the nonparallelism matters in the long run or not then remains to be seen, although clearly it can continually destabilize the boundary layer and bring in the influence of external pressure gradients for instance. In any case, the scales reflect the property that one of the strongest vortex effects arises from the slow decay of the 3DTS waves' amplitudes at the edge of the viscous lower deck or critical layer. Thus the spanwise TS velocity (w) there decays as the inverse of the normal distance y from the surface, and so the inertial response at second order is like y^{-2}. This must balance the main viscous force $\propto \partial^2 w/\partial y^2$ of the induced vortex, implying that the vortex w-component grows logarithmically with y. As a result, substantial vortex motion occurs well outside the viscous TS layer. That substantial motion spreads way out across the boundary layer and

beyond, although its dominant nonlinear interaction effects with the TS flow turn out to spread no further initially than a thin buffer zone lying just outside the lower deck but within the boundary layer: see Figure 1 later. The scales can be derived in a number of ways, we note, for example as in Section 2 or by starting from 3D triple-deck theory and working outwards, as it were. The resulting flow structure found captures the original notion of TS/vortex interaction in the form

$$E_1 E_2^{-1} = E_3 \tag{1.1}$$

where $E_{1,2}$ represent the oblique TS waves and E_3 represents the induced vortex, specifically $E_{1,2} \equiv \exp[i(\alpha X \pm \beta Z/2 - \Omega T)]$ and $E_3 \equiv \exp(i\beta Z)$ in the later notation. The TS-squared forcing of the vortex motion takes place both in the buffer layer and in the lower deck whereas the vortex reaction back on the TS waves is concentrated in the lower-deck flow. The production of the spanwise subharmonics $E_{1,2}$ here is in line with Aihara and Koyama's (1981) experimental findings in vortex break-up.

The interaction equations are summarized and addressed numerically and analytically in Section 5. Certain of the nonlinear properties found appear to agree qualitatively with the Srivastava and Dallmann (1987) approximations a little and with the Aihara and Koyama (1981) experiments, but others do not. A point here with regard to the experimental comparisons is that the theory, being a first step (see earlier comments), deals with a first nonlinear-interaction stage occurring at low amplitudes. Second stages corresponding to higher amplitudes can arise either as a downstream development from the present stage or as a consequence of increased input amplitude upstream. Second stages are indicated directly by the current analysis, as the further discussion in Section 6 describes, and the second-stage interactions can have shorter or longer streamwise extent, depending on the input conditions and the spanwise wavenumbers.

The velocities $u_\infty(u, v, w)$, corresponding Cartesian coordinates $\ell_\infty(x, y, z)$ and pressure $\rho_\infty u_\infty^2 p$ are used, based on the airfoil chord ℓ_∞, free-stream speed u_∞ in the x-direction and the incompressible fluid density ρ_∞, with time written as $u_\infty^{-1}\ell_\infty t$. To fix matters, we may consider usually the flat plate ($y = 0$ for $0 \leq x \leq 1$) with zero pressure gradient, giving a basic Blasius boundary layer with normalized skin-friction factor $\lambda = 0.332\, x_0^{\frac{1}{2}}$ at the typical station $(x, z) = (x_0, z_0)$ under consideration. The extension to nonzero pressure gradients, for example, is referred to in Section 6, and the extensions to nonzero Görtler numbers for curved surfaces and to the compressible regime are also of much interest. The terms λ_b, μ_a introduced later are higher-order corrections of the basic velocity profile. Also, $Re \equiv u_\infty \ell_\infty \nu_\infty^{-1} (= \varepsilon^{-8})$ is the global Reynolds number, with ν_∞ being the kinematic viscosity of the fluid, the superscript * denotes a complex conjugate and r, i stand for the real and imaginary parts of a quantity.

2. THE SCALES AND THE MAIN-DECK RESPONSE

There are several ways to arrive at the scales controlling the 3D TS/induced-vortex nonlinear interaction of present interest. One is as follows: see also Fig. 1. Linear or nonlinear 2D and 3D TS waves are viscous-inviscid interactive phenomena, governed primarily by the triple-deck structure and hence by the unsteady interactive boundary-layer equations holding in the lower deck which has y-extent $0(\varepsilon^5)$ near the wall (Smith, 1979a). If the 3DTS amplitudes are comparatively small, say of order h relative to the fully nonlinear sizes, then inertial effects force a vortex motion at relative order h^2. The spanwise inertial effects ($u\partial w/\partial x$, etc.) in particular decay only slowly, however, like Y^{-2}, with scaled distance Y from the wall, due to the algebraic decay of the 3DTS velocities into their asymptotes, and so the spanwise velocity (w_v) of the induced vortex grows logarithmically like ℓnY (Hall and Smith, 1984) since the vortex response is predominantly viscous here. This growth is then damped down further away from the wall where $Y \sim \delta(\gg 1)$ say in a buffer zone and the relatively slow streamwise variation of the vortex takes effect, introducing the comparatively slow inertial operator $Y\partial_{\overline{X}}$ [from the boundary-layer shear] to combat the viscous one ∂_Y^2. So $\partial_{\overline{X}}$ is $0(\delta^{-3})$. There w_v is of relative order $h^2\ell n\delta$, provoking by continuity a streamwise velocity u_v of relative order $h^2\delta^3\ell n\delta$ typically, in the vortex, which therefore alters the basic shear by a relative amount of the order $h^2\delta^2\ell n\delta$. The relative influences of the slow streamwise modulation $\sim \delta^{-3}$ and the change in mean shear $\sim h^2\delta^2\ell n\delta$ above are in balance if $\delta \sim h^{-\frac{2}{5}}$, to within a logarithmic factor, and this balance is central to the nonlinear evolution of the provoked vortex flow and the TS disturbance. Another feature that needs to be considered is the effect of nonparallelism in the basic flow, due to the boundary-layer divergence among other things. Nonparallelism affects the TS and vortex interaction over unscaled streamwise lengths typically of order δ^{-3} since that is the characteristic amount by which the critical linear conditions are disturbed in the vortex-TS interaction above. On the other hand, the unscaled length associated with the streamwise modulation of the TS wave or vortex is $0(\varepsilon^3\delta^3)$ because the triple-deck length scale is $0(\varepsilon^3)$. Hence nonparallel-flow effects are accommodated in the balance $\varepsilon^3\delta^3 \sim \delta^{-3}$, giving $\delta \sim \varepsilon^{\frac{1}{2}}$, which is large as assumed initially. Nonparallelism would be negligible for $\delta \ll \varepsilon^{-\frac{1}{2}}$, but the stage to be addressed here, namely

$$\delta \sim \varepsilon^{-\frac{1}{2}},\ h \sim \varepsilon^{\frac{5}{4}}, \tag{2.1a}$$

is possibly a crucial one in our opinion as it marks the intrusion of significant nonparallel-flow effects and hence of more global properties into the nonlinear TS-vortex interaction. (We remark here that the scales in (2.1a) can be inferred from Hall and Smith (1984), and also if the induced vortex is absent the disturbance size required to bring in nonparallelism

is raised to $h \sim \varepsilon^{\frac{5}{4}}$). Whether the nonparallelism thus captured by (2.1a) actually has a substantial impact on the interaction or not can only be decided by the solution properties of the resulting nonlinear governing equations. One inner limit of these equations reproduces the parallel-flow version of the TS-vortex interaction in any case. With the suggested scales (2.1a) holding, then, the scene is set for a multi-scaling in which

$$\partial_t \to \varepsilon^{-2}\partial_T,\ \partial_x \to \varepsilon^{-3}\partial_X + \varepsilon^{-\frac{3}{2}}\partial_{\overline{X}},\ \partial_z \to \varepsilon^{-3}\partial_Z, \tag{2.1b}$$

where $(t, x - x_0, z - z_0) = (\varepsilon^2 T, \varepsilon^3 X, \varepsilon^3 Z)$ define the main 3DTS time and length scales, $x - x_0 = \varepsilon^{\frac{3}{2}}\overline{X}$ defines the slower modulation scale of the TS waves and the induced-vortex flow, and four y-scales come into operation:

$$y = \varepsilon^3 y',\ \varepsilon^4\overline{y},\ \varepsilon^{\frac{9}{2}}\hat{y},\ \varepsilon^5 Y. \tag{2.1c}$$

The $\varepsilon^3, \varepsilon^4, \varepsilon^5$ levels are associated with the three decks of the triple-deck TS structure, while the extra level $\varepsilon^{\frac{9}{2}}$ is necessary for the determination of the forced vortex motion because of (2.1a). The scales (2.1a) also indicate that the amplitudes involved in nonlinear TS-vortex interaction are quite small, initially at least, with a typical TS pressure or free-stream-disturbance amplitude of order $\varepsilon^2 h$, i.e., $\varepsilon^{\frac{13}{4}}$, and an induced-vortex spanwise velocity w of the size $\varepsilon h^2 \ell n(h)$, i.e., $\varepsilon^{\frac{7}{2}}\ell n\varepsilon$, at most.

The flow properties in the four decks are examined below in this section, for the main deck, in Section 3, for the buffer and lower decks, and in Section 4 for the upper deck. Since nonparallel-flow effects are incorporated for completeness, certain extra features arise including the basic-flow expansion profiles $\overline{X}\overline{u}_b(\overline{y}), \overline{v}_b(\overline{y})$ (i.e., $u = \overline{u} + (x - x_0)\overline{u}_b + \cdots, v = \overline{v}_b + \cdots$) satisfying the steady boundary-layer balance $\overline{u}_b + \overline{v}_b' = 0, \overline{u}\ \overline{u}_b + \overline{v}_b\overline{u}' = \overline{u}''$, and $\lambda_b \equiv \overline{u}_b'(0)$.

In the main deck the unsteady 3D flow solution expands in the pattern

$$u = \overline{u}(\overline{y}) + \varepsilon^{\frac{3}{2}}\overline{X}\overline{u}_b(\overline{y}) + \varepsilon^2\overline{u}^{(3)} + \varepsilon^{\frac{9}{4}}\overline{u}^{(1)} + \cdots + \varepsilon^{\frac{13}{4}}\overline{\overline{u}} + \varepsilon^{\frac{15}{4}}\overline{u}^{(e)} + \cdots, \tag{2.2a}$$

$$v = \varepsilon^{\frac{13}{4}}\overline{v}^{(1)} + \varepsilon^4\overline{v}_b + \varepsilon^{\frac{17}{4}}\overline{\overline{v}} + \varepsilon^{\frac{9}{2}}\overline{v}^{(3)} + \cdots + \varepsilon^{\frac{19}{4}}\overline{v}^{(e)} + \cdots, \tag{2.2b}$$

$$w = \varepsilon^{\frac{13}{4}}\overline{w}^{(1)} + \varepsilon^{\frac{17}{4}}\overline{\overline{w}} + \varepsilon^{\frac{9}{2}}\overline{w}_{3E} + \varepsilon^{\frac{19}{4}}\overline{w}^{(e)} + \cdots + \varepsilon^5\overline{w}^{(3)} + \cdots, \tag{2.2c}$$

$$p = \varepsilon^{\frac{13}{4}}\overline{p}^{(1)} + \varepsilon^{\frac{19}{4}}\overline{p}^{(e)} + \cdots + \varepsilon^6\overline{p}^{(3)} + \cdots \tag{2.2d}$$

essentially. Here $y = \varepsilon^4\overline{y}$, the superscript (3) denotes the induced vortex flow, which is independent of the fastest streamwise and temporal scales X, T, the superscript (1) refers to the main TS contributions present, while the double overbar denotes higher-order TS effects. The contributions $\overline{p}^{(3)}, \overline{w}_{3E}$ and similar higher-order terms in u, v are forced by the induced-vortex flow outside the boundary-layer as explained in Section 4 below. Also, (e)

signifies the extra TS contributions affected by the nonparallelism ($\propto \overline{u}_b, \overline{v}_b$ in (2.2a,b)). The governing equations for the successive terms above are obtained from substitution into the Navier-Stokes equations and are as follows.

First, the dominant TS waves satisfy continuity and momentum equations which are quasi-steady and show the pressure variation across the boundary layer to be negligible:

$$\overline{u}_X^{(1)} + \overline{v}_{\overline{Y}}^{(1)} = 0, \ \overline{u}\,\overline{u}_X^{(1)} + \overline{v}^{(1)}\overline{u}' = 0, \tag{2.3a,b}$$

$$0 = -\overline{p}_{\overline{Y}}^{(1)}, \ \overline{u}\,\overline{w}_X^{(1)} = -\overline{p}_Z^{(1)}. \tag{2.3c,d}$$

These yield the expected displacement-effect solutions

$$\overline{u}^{(1)} = (A_{11}E_1 + A_{12}E_2)\overline{u}' + c.c., \tag{2.4a}$$

$$\overline{v}^{(1)} = -i\alpha(A_{11}E_1 + A_{12}E_2)\overline{u} + c.c., \tag{2.4b}$$

$$\overline{p}^{(1)} = (\overline{p}_{11}E_1 + \overline{p}_{12}E_2) + c.c., \tag{2.4c}$$

$$\overline{w}^{(1)} = (\overline{w}_{11}E_1 + \overline{w}_{12}E_2) + c.c. : \ \overline{w}_{11,12} = \mp\beta\overline{p}_{11,12}/2\alpha\overline{u}, \tag{2.4d}$$

where c.c. denotes the complex conjugate and all the fast dependence on X, T is contained in the two oblique waves

$$E_{1,2} \equiv \exp[i(\alpha X \pm \beta Z/2 - \Omega T)]. \tag{2.5}$$

Here the TS wavenumbers $\alpha, \beta/2$ and frequency Ω are real (see (3.14) below), and the displacement decrements A_{11}, A_{12} and pressure components $\overline{p}_{11}, \overline{p}_{12}$ are unknown functions of $\overline{X}$.

Next, the higher-order TS influences represented by double-overbarred and (e) terms in (2.2) are controlled effectively by forced versions of the main TS balances (2.3) accounting for unsteadiness and nonparallelism. These yield in particular

$$\overline{u}^{(e)} = \overline{u}_{e1}E_1 + \overline{u}_{e2}E_2 + c.c. \tag{2.6a}$$

and so on, where

$$\overline{u}_{e1} = A_{e1}\overline{u}' + A_{11}\overline{X}\overline{u}_b', \tag{2.6b}$$

$$\overline{v}_{e1} = -(i\alpha A_{e1} + A_{11\overline{X}})\overline{u} - i\alpha A_{11}\overline{X}\overline{u}_b, \tag{2.6c}$$

with $-A_{e1}$ representing an extra displacement correction which again is unknown in advance. These influences are of little significance at this stage.

The induced-vortex motion here in the main desk is also fairly passive, merely responding to the efflux ($\propto A_{33}$) from the buffer layer examined in the next section. Thus the

governing equations for $\overline{u}^{(3)}, \overline{v}^{(3)}, \overline{w}_{3E}, \overline{p}^{(3)}$ are analogous to those for the dominant TS wave but on the slower $\overline{X}$ scale and give the solutions

$$\overline{u}^{(3)} = A_{33}E_3\overline{u}' + c.c., \ \overline{v}^{(3)} = -A_{33\overline{X}}E_3\overline{u} + c.c. \qquad (2.7a,b)$$

$$\overline{p}^{(3)} = \overline{p}_{33}(\overline{X})E_3 + c.c., \ \overline{w}_{3E} = \overline{D}_{3E}(\overline{X})E_3/\overline{u} + c.c. \qquad (2.7c,d)$$

where $\overline{D}_{3E}$ satisfies $\partial\overline{D}_{3E}/\partial\overline{X} = -i\beta\overline{p}_{33}$, the vortex pressure $\overline{p}_{33}$ is an unknown function of $\overline{X}$, as is the vortex displacement $-A_{33}$, and the spanwise dependence of the vortex is on

$$E_3 \equiv \exp(i\beta Z). \qquad (2.8)$$

Significant vortex-TS interaction does not occur in the main deck and is confined instead to the lower reaches of the boundary layer, specifically in the buffer and lower decks which are discussed in the subsequent section. The nonlinear interaction arises from inertial interplay which produces the combinations

$$E_1E_2^{-1} = E_3, \ E_3E_2 = E_1, \ E_3^{-1}E_1 = E_2, \qquad (2.9)$$

thus enabling the two oblique TS waves to force the vortex motion, and the vortex, combined with one TS wave, to force the other TS wave, at the amplitude-squared level. In addition, the enhanced vortex-TS interaction near the wall is due to the increase in the TS spanwise motion there as represented by the singular behavior of $\overline{w}^{(1)}$ in (2.4) as $\overline{y} \to 0+$, as well as by the higher-order TS effects, a singular response which is smoothed out in the viscous lower deck.

3. THE BUFFER DECK AND THE LOWER DECK

(a) The buffer.

This extra, buffer, deck of width $0(\varepsilon^{\frac{9}{2}})$ in y is brought into action because it controls the major response of the induced vortex flow, due in turn to the algebraic decay of the 3DTS waves on exit from the lower deck, i.e. their growth in the lower extremes of the main deck. The buffer deck has the underlying pattern

$$u = \varepsilon^{\frac{1}{2}}\lambda\hat{y} + \varepsilon^2[\overline{X}\lambda_b\hat{y} + \mu_a\hat{y}^4 + \hat{u}^{(3)}] + \cdots + \varepsilon^{\frac{9}{4}}\hat{u}^{(1)} + \cdots + \varepsilon^{\frac{11}{4}}\hat{\hat{u}} + \cdots + \varepsilon^{\frac{15}{4}}\hat{u}^{(e)} + \cdots, \qquad (3.1a)$$

$$v = \varepsilon^{\frac{15}{4}}\hat{v}^{(1)} + \varepsilon^{\frac{17}{4}}\hat{\hat{v}} + \varepsilon^5[-\lambda_b\hat{y}^2/2 + \hat{v}^{(3)}] + \cdots + \varepsilon^{\frac{21}{4}}\hat{v}^{(e)} + \cdots, \qquad (3.1b)$$

$$w = \varepsilon^{\frac{11}{4}}\hat{w}^{(1)} + \varepsilon^{\frac{13}{4}}\hat{\hat{w}} + \varepsilon^{\frac{7}{2}}\ell n\varepsilon\hat{w}_L^{(3)} + \varepsilon^{\frac{7}{2}}\hat{w}^{(3)} + \varepsilon^{\frac{17}{4}}\hat{w}^{(e)} + \cdots, \qquad (3.1c)$$

$$p = \varepsilon^{\frac{13}{4}}\hat{p}^{(1)} + \varepsilon^{\frac{19}{4}}\hat{p}^{(e)} + \cdots + \varepsilon^6\hat{p}^{(3)} + \cdots, \qquad (3.1d)$$

where now $y = \varepsilon^{\frac{9}{2}}\hat{y}$, these expansions being implied mostly by the behavior of the solutions in the main deck for small $\overline{y}$ but partly also by the lower-deck features discussed subsequently.

The governing equations for the dominant TS disturbance $\hat{u}^{(1)}$, etc., are merely the continuations of those in Section 2, in fact, so that

$$\hat{u}^{(1)} = \lambda(A_{11}E_1 + A_{12}E_2) + c.c., \ \hat{v}^{(1)} = -i\alpha\lambda\hat{y}(A_{11}E_1 + A_{12}E_2) + c.c., \qquad (3.2a,b)$$

$$\hat{p}^{(1)} = (\hat{p}_{11}E_1 + \hat{p}_{12}E_2) + c.c., \ \hat{w}^{(1)} = \beta(-\hat{p}_{11}E_1 + \hat{p}_{12}E_2)/2\lambda\alpha\hat{y} + c.c. \qquad (3.2c,d)$$

with $\hat{p}_{11} = \overline{p}_{11}, \hat{p}_{12} = \overline{p}_{12}$. Likewise the nonparallel effect here is given simply by

$$\hat{u}^{(e)} = \lambda A_e + (\overline{X}\lambda_b + \hat{u}^{(3)}_{\hat{y}})A_1, \qquad (3.3a)$$

$$\hat{v}^{(e)} = -(A_{eX} + A_{1\overline{X}})\lambda\hat{y} - A_{1X}\overline{X}\lambda_b\hat{y} - A_{1X}\hat{u}^{(3)}, \qquad (3.3b)$$

and the higher-order TS contributions continue the trend of algebraic growth, in the form

$$\hat{\hat{u}} = \beta^2(\hat{p}_{11}E_1 + \hat{p}_{12}E_2)/4\lambda\alpha^2\hat{y} + c.c., \qquad (3.4a)$$

$$\hat{\hat{v}} = i(\Omega A_{11} - \beta^2\hat{p}_{11}/4\alpha\lambda - \alpha\hat{p}_{11}/\lambda)E_1 + i(\Omega A_{12} - \beta^2\hat{p}_{12}/4\alpha\lambda - \alpha\hat{p}_{12}/\lambda)E_2 + c.c., \qquad (3.4b)$$

$$\hat{\hat{w}} = \Omega\hat{w}^{(1)}/\alpha\lambda\hat{y}. \qquad (3.4c)$$

These last contributions play a vital role nonlinearly, however, in the generation and evolution of the longitudinal vortex motion, through the major inertial response which is given by

$$\hat{u}^{(1)}\hat{\hat{w}}_X + \hat{\hat{u}}\hat{w}^{(1)}_X + \hat{v}^{(1)}\hat{\hat{w}}_{\hat{y}} + \hat{\hat{v}}\hat{w}^{(1)}_{\hat{y}} + \hat{w}^{(1)}\hat{w}^{(1)}_Z$$

in the spanwise momentum balance, i.e., by $E_3\hat{p}_{11}\hat{p}^*_{12}i\beta(4\alpha^2 - \beta^2)/4\alpha^2\lambda^2\hat{y}^2$, from (3.2), (3.4) along with (2.9), as far as the vortex is concerned. The lower-order contribution $\hat{u}^{(1)}\hat{w}^{(1)}_X + \hat{v}^{(1)}\hat{w}^{(1)}_{\hat{y}}$ cancels out, we note, and the logarithmic vortex effect $\hat{w}^{(3)}_L$, etc., is only a passive one, discussion of which can be deferred for now. Thus the vortex motion of concern is controlled by the forced viscous-inviscid equations

$$\hat{u}_{33\overline{X}} + \hat{v}_{33\hat{y}} + i\beta\hat{w}_{33} = 0, \qquad (3.5a)$$

$$\lambda\hat{y}\hat{u}_{33\overline{X}} + \lambda\hat{v}_{33} = \hat{u}_{33\hat{y}\hat{y}}, \qquad (3.5b)$$

$$\lambda\hat{y}\hat{w}_{33\overline{X}} + i\beta(1 - \beta^2/4\alpha^2)\overline{p}_{11}\overline{p}^*_{12}/\lambda^2\hat{y}^2 = \hat{w}_{33\hat{y}\hat{y}}, \qquad (3.5c)$$

where we split $\hat{u}^{(3)} \to \hat{u}_{33}E_3 + c.c.$ and so on. The boundary conditions on this vortex flow are to match, respectively, with the main-deck behavior for large $\hat{y}$ and with the lower deck for small $\hat{y}$:

$$\hat{u}_{33} \to \lambda A_{33}, \ \hat{v}_{33} \sim -\lambda A_{33\overline{X}}\hat{y}, \ \hat{w}_{33} \propto \hat{y}^{-3}, \text{ as } \hat{y} \to \infty \qquad (3.5d)$$

$$\hat{u}_{33} = \hat{v}_{33} = 0 \text{ at } \hat{y} = 0,\ \hat{w}_{33} \sim -i\beta(1-\beta^2/4\alpha^2)\lambda^{-2}\overline{p}_{11}\overline{p}^*_{12}\ell n\hat{y} + \Phi(\overline{X}) \text{ as } \hat{y} \to 0+. \quad (3.5e)$$

Here the term Φ in $\hat{w}_{33}$ in (3.5e) is unknown as yet and has to be determined by the lower-deck response, as examined below, while the logarithmic term forces corresponding effects $\propto \hat{y}\ell n\hat{y},\ \hat{y}^3\ell n\hat{y}$ in $\hat{v}_{33},\ \hat{u}_{33}$ as $\hat{y}$ tends to zero. All these effects merge with those of the lower deck. The main feature that the induced vortex motion imposes on the lower-deck behavior is the skin-friction modification, $\hat{u}_{33} \sim \hat{\lambda}_{33}\hat{y}$ as $\hat{y} \to 0+$ where

$$\lambda_{33}(\overline{X}) \equiv \partial_{\hat{y}}\hat{u}_{33}(\overline{X}, 0), \quad (3.6)$$

but that depends on the TS-induced forcing $\overline{p}_{11}\overline{p}^*_{12}$ in (3.5c) and Φ in (3.5e) which in turn depend on the skin-friction modification λ_{33} (see below), so that the whole process is highly interactive.

Further points of note here concern: the extra logarithmic effects in (3.1); the fact that viscosity affects the vortex motion in the buffer zone; the pure displacement effect in (3.5d) and the feature that the pressure feedback from the upper deck due to $A_{33}E_3(+\text{ c.c.})$ is negligible in (3.5b,c); and how the entire structure might be affected by pressure gradients or cross-flow. These points are addressed subsequently.

The logarithmically larger vortex effects $\hat{w}^{(3)}_L$ and corresponding terms in u, v satisfy (3.5a-c) again, but with 33 replaced by 33L when the split $\hat{w}^{(3)}_L \to \hat{w}_{33L}E_3+$ c.c. is applied and with the forcing term $\propto \overline{p}_{11}\overline{p}^*_{12}$ absent. The appropriate boundary conditions then are $\hat{w}_{33L} = \hat{\gamma}, \hat{u}_{33L} = \hat{v}_{33L} = \partial\hat{u}_{33L}/\partial\hat{y} = 0$ at $\hat{y} = 0$ and $\hat{w}_{33L} \to 0,\ \partial\hat{u}_{33L}/\partial\hat{y} \to 0$ as $\hat{y} \to \infty$, where the sole forcing term $\hat{\gamma} \equiv i\beta(1-\beta^2/4\alpha^2)\lambda^{-2}\overline{p}_{11}\overline{p}^*_{12}/2$ because of the lower-deck spanwise response in (3.18d) below (with $Y \to \varepsilon^{-\frac{1}{2}}\hat{y}$) and the zero-shear condition on $\hat{u}_{33L}$ is required to merge the buffer- and lower-deck induced shears. The solution here is de-coupled in effect from the dominant TS-vortex interaction. Thus the solution for $\hat{w}_{33L}$ can be written formally in terms of a Fourier or Laplace transform in $\overline{X}$ and an Airy function, giving the required decay at large $\hat{y}$, while the shear $\hat{\tau}_{33L} \equiv \partial\hat{u}_{33L}/\partial\hat{y}$ is governed by the same equation as is $\hat{w}_{33L}$ except for a forcing $\lambda i\beta\hat{w}_{33L}$, and subject to $\hat{\tau}_{33L}$ vanishing at $\hat{y} = 0$ and as $\hat{y} \to \infty$, the transform solution for $\hat{\tau}_{33L}$ therefore being a combination of the Airy function and its derivative. Integration with respect to $\hat{y}$, subject to $\hat{u}_{33L}$ vanishing at $\hat{y} = 0$, then yields $\hat{u}_{33L}$ for all $\hat{y}$ and the displacement correction, A_{33L} say, emerges from the large-$\hat{y}$ value of $\hat{u}_{33L}$. Hence the logarithmic ($\ell n\varepsilon$) parts of the induced vortex motion here play only a passive part.

b. The lower deck

The lower deck, of width $0(\varepsilon^5)$ and containing the critical layer, lies beneath the buffer and brings in viscous forces to reduce the TS flow to rest at the wall. This smoothing of

the TS distributions in turn serves to smooth out the forced vortex response, in particular modifying the logarithmic irregularities connected with (3.5e) for small $\hat{y}$. In the lower deck, where $y = \varepsilon^5 Y$ say, the flow solution can be expressed in the form

$$u = \varepsilon\lambda Y + \varepsilon^{\frac{9}{4}}\tilde{u}^{(1)} + \varepsilon^{\frac{5}{2}}[\lambda_3 Y + \overline{X}\lambda_b Y] + \varepsilon^{\frac{7}{2}}\tilde{u}^{(3)} + \varepsilon^{\frac{15}{4}}\tilde{u}^{(e)} + 0(\varepsilon^4 Y^2) + \cdots, \tag{3.7a}$$

$$v = \varepsilon^{\frac{17}{4}}\tilde{v}^{(1)} + \varepsilon^{\frac{11}{2}}\tilde{v}^{(3)} + \varepsilon^{\frac{23}{4}}\tilde{v}^{(e)} - \varepsilon^6\lambda_b Y^2/2 + \cdots, \tag{3.7b}$$

$$w = \varepsilon^{\frac{9}{4}}\tilde{w}^{(1)} + \varepsilon^{\frac{7}{2}}\tilde{w}^{(3)} + \varepsilon^{\frac{15}{4}}\tilde{w}^{(e)} + \cdots, \tag{3.7c}$$

$$p = \varepsilon^{\frac{13}{4}}\tilde{p}^{(1)} + \varepsilon^{\frac{19}{4}}\tilde{p}^{(e)} + \cdots + \varepsilon^6\tilde{p}^{(3)} + \cdots, \tag{3.7d}$$

with λ_3 denoting $\lambda_{33}E_3+$ c.c. The induced-vortex components are principally the shear contribution $\lambda_3 Y$ (produced via the buffer) and the more complicated parts $\tilde{u}^{(3)}, \tilde{v}^{(3)}, \tilde{w}^{(3)}$, whereas the main TS components have superscript (1) again. The continuity, streamwise momentum and spanwise momentum balances then yield, successively, and in view of the interplay in (2.9),

$$\begin{cases} \tilde{u}^{(1)}_X + \tilde{v}^{(1)}_Y + \tilde{w}^{(1)}_Z = 0, \ \tilde{u}^{(e)}_X + \tilde{u}^{(1)}_{\overline{X}} + \tilde{v}^{(e)}_Y + \tilde{w}^{(e)}_Z = 0, \\ \tilde{v}^{(3)}_Y + w^{(3)}_Z = 0; \end{cases} \tag{3.8a-c}$$

$$\begin{cases} \tilde{u}^{(1)}_T + \lambda Y\tilde{u}^{(1)}_X + \tilde{v}^{(1)}\lambda = -\tilde{p}^{(1)}_X + \tilde{u}^{(1)}_{YY}, \\ \tilde{u}^{(e)}_T + \lambda Y(\tilde{u}^{(e)}_X + \tilde{u}^{(1)}_{\overline{X}}) + (\overline{X}\lambda_b Y + \lambda_3 Y)\tilde{u}^{(1)}_X + \tilde{v}^{(1)}(\lambda_3 + \overline{X}\lambda_b) + \tilde{v}^{(e)}\lambda \\ \quad = -\tilde{p}^{(e)}_X - \tilde{p}^{(1)}_{\overline{X}} + \tilde{u}^{(e)}_{YY}, \\ \tilde{u}^{(1)}\tilde{u}^{(1)}_X + \tilde{v}^{(3)}\lambda + \tilde{v}^{(1)}\tilde{u}^{(1)}_Y + \tilde{w}^{(1)}\tilde{u}^{(1)}_Z = \tilde{u}^{(3)}_{YY}; \end{cases} \tag{3.9a-c}$$

$$\begin{cases} \tilde{w}^{(1)}_T + \lambda Y\tilde{w}^{(1)}_X = -\tilde{p}^{(1)}_Z + \tilde{w}^{(1)}_{YY}, \\ \tilde{w}^{(e)}_T + \lambda Y(\tilde{w}^{(e)}_X + \tilde{w}^{(1)}_{\overline{X}}) + (\overline{X}\lambda_b Y + \lambda_3 Y)\tilde{w}^{(1)}_X = -\tilde{p}^{(e)}_Z + \tilde{w}^{(e)}_{YY}, \\ \tilde{u}^{(1)}\tilde{w}^{(1)}_X + \tilde{v}^{(1)}\tilde{w}^{(1)}_Y + \tilde{w}^{(1)}\tilde{w}^{(1)}_Z = \tilde{w}^{(3)}_{YY}, \end{cases} \tag{3.10a-c}$$

for the main TS, the forced TS and the vortex flow, in turn, all three of which need to be addressed below. Only the E_3 components are of concern in (3.9c), (3.10c), we note, and the y-momentum balance requires the pressure effects shown in (3.7d) to be independent of Y, leaving the results $\tilde{p}^{(1)} = \hat{p}^{(1)} = \overline{p}^{(1)}, \tilde{p}^{(e)} = \hat{p}^{(e)} = \overline{p}^{(e)}, \tilde{p}^{(3)} = \hat{p}^{(3)} = \overline{p}^{(3)}$.

Splitting the TS responses into their pairs of oblique waves and the vortex into its spanwise parts now, so that

$$\tilde{u}^{(1)} = \tilde{u}_{11}E_1 + \tilde{u}_{12}E_2 + c.c., \ \tilde{u}^{(e)} = \tilde{u}_{e1}E_1 + \tilde{u}_{e2}E_2 + c.c., \ \tilde{u}^{(3)} = \tilde{u}_{33}E_3 + c.c. \tag{3.11}$$

and so on, we have from (3.8a), (3.9a), (3.10a) the governing equations

$$i\alpha\tilde{u}_{1n} + \tilde{v}_{1nY} \pm i\beta\tilde{w}_{1n}/2 = 0, \tag{3.12a}$$

$$-i\Omega\tilde{u}_{1n} + i\alpha\lambda Y\tilde{u}_{1n} + \lambda\tilde{v}_{1n} = -i\alpha\overline{p}_{1n} + \tilde{u}_{1nYY}, \tag{3.12b}$$

$$-i\Omega\tilde{w}_{1n} + i\alpha\lambda Y\tilde{w}_{1n} = \mp i\beta\overline{p}_{1n}/2 + \tilde{w}_{1nYY}, \tag{3.12c}$$

for the main TS wave, for $n = 1, 2$ respectively, subject to the constraints of no slip at the wall, of matching with the buffer solution and of pressure-displacement interaction:

$$\tilde{u}_{1n} = \tilde{v}_{1n} = \tilde{w}_{1n} = 0 \text{ at } Y = 0, \tag{3.12d}$$

$$\tilde{u}_{1n} \to \lambda A_{1n}, \ \tilde{w}_{1n} \to 0(Y^{-1}) \text{ as } Y \to \infty, \tag{3.12e}$$

$$(\alpha^2 + \beta^2/4)^{\frac{1}{2}}\overline{p}_{1n} = \alpha^2 A_{1n}. \tag{3.12f}$$

Here (3.12f) anticipates the results of Section 4. The solution of the linear TS problem (3.12a-f) can be expressed in terms of the Airy function Ai and leads to the eigenrelation

$$\lambda^2 Ai'(\xi_0)/\kappa = (i\alpha\lambda)^{\frac{1}{3}}(\alpha^2 + \beta^2/4)^{\frac{1}{2}}, \text{ with } \begin{cases} \xi_0 \equiv -i^{\frac{1}{3}}\Omega/(\alpha^{\frac{2}{3}}\lambda^{\frac{2}{3}}) \\ \kappa \equiv \int_{\xi_0}^{\infty} Ai(s)ds, \end{cases} \tag{3.13}$$

determining α for given real β, Ω values. The required neutral condition corresponds to $\xi_0 = -d_1 i^{\frac{1}{3}}, Ai'(\xi_0)/\kappa = d_2 i^{\frac{1}{3}}[d_1 \approx 2.30, d_2 \approx 1.00]$, however, so that

$$\alpha^{\frac{1}{3}}(\alpha^2 + \beta^2/4)^{\frac{1}{2}} = d_2\lambda^{\frac{5}{3}}, \ \Omega = d_1\alpha^{\frac{2}{3}}\lambda^{\frac{2}{3}} \tag{3.14}$$

relate the real α, β, Ω values of concern here. In the above $i^{\frac{1}{3}}$ denotes $\exp(i\pi/6)$.

Next, the forced TS wave ($\tilde{u}_{e1}$, etc.), driven by the combination of modulation and nonparallel- and vortex-flow effects in (3.8b), (3.9b), (3.10b), satisfies (3.12a-c) again with subscripts 11 replaced by $e1$ of course and with $\tilde{u}_{11\overline{X}}, \lambda Y\tilde{u}_{11\overline{X}} + \overline{X}\lambda_b Y i\alpha\tilde{u}_{11} + \lambda_{33}Y i\alpha\tilde{u}_{12} + \overline{X}\lambda_b\tilde{v}_{11} + \lambda_{33}\tilde{v}_{12} + \overline{p}_{11\overline{X}}, \lambda Y\tilde{w}_{11\overline{X}} + \overline{X}\lambda_b Y i\alpha\tilde{w}_{11} + \lambda_{33}Y i\alpha\tilde{w}_{12}$ added to the respective left-hand sides, for $n = 1$, and similarly for $n = 2$. In addition, the boundary conditions are (3.12d,e) again with $11 \to e1$ and with $\lambda_b\overline{X}A_{11} + \lambda_{33}A_{12}$ supplementing the right-hand side of (3.12e) (for $n = 1$, similarly for $n = 2$), coupled with the interaction law

$$(\alpha^2 + \beta^2/4)^{\frac{1}{2}}\overline{p}_{en} = \alpha^2 A_{en} - 2i\alpha A_{1n\overline{X}} + i\alpha^3 A_{in\overline{X}}/(\alpha^2 + \beta^2/4) \tag{3.15}$$

stemming from the upper-deck properties presented in the next section. This forced-TS system requires a compatibility relation to hold between all the driving effects just

described, and, after some manipulation, the relation is found to provide the governing equations

$$\begin{cases} a\overline{p}_{11\overline{X}} + b\overline{X}\lambda_b\overline{p}_{11} + c\lambda_{33}\lambda^{-1}\overline{p}_{12} = 0, \\ a\overline{p}_{12\overline{X}} + b\overline{X}\lambda_b\overline{p}_{12} + c\lambda^*_{33}\lambda^{-1}\overline{p}_{11} = 0 \end{cases} \qquad (3.16a,b)$$

for the slower-scale modulations of the primary TS pressure amplitudes. In each of (3.16a,b) the second term represents the effects of the nonparallelism of the basic flow while the third term comes from the extra induced-vortex motion (via (3.6)). Also,

$$a = 2B\xi_0 r_1 D/3\alpha\Delta^{\frac{2}{3}} - i\lambda B^{-\frac{1}{2}}(4/3 + \beta^2/12\alpha^2), \qquad (3.17a)$$

$$b = -2\alpha\xi_0 r_1 BD/3\Delta^{\frac{5}{3}} - 5B^{\frac{1}{2}}/3\alpha, \qquad (3.17b)$$

$$c = iD\xi_0\Delta^{-\frac{2}{3}}(2Br_1/3 + \beta^2 r_2/8) - \lambda\alpha^{-1}B^{-\frac{1}{2}}(5\alpha^2/3 + \beta^2/24), \qquad (3.17c)$$

where $D \equiv 1+\kappa\xi_0/Ai'(\xi_0), B \equiv \alpha^2+\beta^2/4, \Delta \equiv i\alpha\lambda, r_1 \equiv Ai(\xi_0)/Ai'(\xi_0), r_2 = \kappa/Ai(\xi_0)$. An origin shift in terms of $\overline{X}$ is implicit in the above to account for the sub- or super-criticality of the flow.

Finally here, the induced vortex flow in the lower deck is controlled by (3.8c), (3.9c), (3.10c) with (3.11). But the spanwise balance (3.10c) alone is sufficient in fact to pin down the most significant unknown property, the viscous TS-amplitude-squared contribution (or jump term) $\Phi(\overline{X})$ which is required to complete the prescription of the induced vortex motion in (3.5). Thus, taking the E_3 component in (3.10c), we have to solve

$$\tilde{w}''_{33} = -i\alpha\tilde{u}_{11}\tilde{w}^*_{12} + i\alpha\tilde{u}^*_{12}\tilde{w}_{11} + \tilde{v}_{11}\tilde{w}^{*\prime}_{12} + \tilde{v}^*_{12}\tilde{w}'_{11} + i\beta\tilde{w}^*_{12} \qquad (3.18a)$$

for $\tilde{w}_{33}(\overline{X}, Y)$, subject to no slip at the wall and to joining with the buffer deck:

$$\tilde{w}_{33} = 0 \text{ at } Y = 0, \qquad (3.18b)$$

$$\tilde{w}'_{33} \to 0 \text{ as } Y \to \infty, \qquad (3.18c)$$

$$\Rightarrow \tilde{w}_{33} \sim -i\beta(1 - \beta^2/4\alpha^2)\lambda^{-2}\overline{p}_{11}\overline{p}^*_{12}\ell nY + \Phi(\overline{X}) \text{ as } Y \to \infty. \qquad (3.18d)$$

The logarithmic behavior here, arising from the algebraic decay of the 3DTS velocities involved on the right of (3.18a) into their large-Y asymptotes (from (3.12)), matches with the corresponding logarithmic responses present in (3.1), (3.5), and similarly for $\tilde{u}_{33}, \tilde{v}_{33}$. Further, in view of the nonlinear forcing in (3.18a),the jump term Φ can be written

$$\Phi = \phi\overline{p}_{11}\overline{p}^*_{12} \qquad (3.19)$$

where ϕ is a constant to be determined, for prescribed β. Relevant comments at this stage are the following. First, we need the complete behavior $0(\ell nY) + 0(1)$ in (3.18d) to feed as

a boundary condition into the main vortex problem (3.5) in the buffer. Thus, the whole balance between the buffer and lower decks is interactive. Second, some of the solution here follows by taking a limit of the Hall and Smith (1984) analysis to deal with standing waves. Third, a nonzero basic pressure gradient adds an $\varepsilon^2 Y^2$ term to u, which is a minor effect on the vortex; see also Section 6. Fourth, the pressure $\varepsilon^6 \tilde{p}_3$ is induced through the upper-deck interaction, due to displacement: see the next section. Fifth, the effects of the induced vortex and of the basic-flow nonparallelism are comparable here and in the buffer.

4. THE PRESSURE-DISPLACEMENT INTERACTIONS VIA THE UPPER DECK

The upper deck lies outside the boundary layer and has a y-scale of $0(\varepsilon^3)$, within which linearized potential-flow properties act to link together the various pressure and displacement distributions present. The velocity and pressure fields here have

$$(u,v,w,p) = (1,0,0,0) + \varepsilon^{\frac{13}{4}}(u^{(1)},v^{(1)},w^{(1)},p^{(1)}) + \varepsilon^{\frac{19}{4}}(u^{(e)},v^{(e)},w^{(e)},p^{(e)})$$

$$+(\varepsilon^6 u^{(3)},\varepsilon^{\frac{9}{2}}v^{(3)},\varepsilon^{\frac{9}{2}}w^{(3)},\varepsilon^6 p^{(3)}) + \cdots, \tag{4.1}$$

where the terms on the right-hand side represent, in order, the uniform external stream, the main TS wave, the extra forced TS wave and the induced vortex. The disparity in the vortex velocity sizes is due to the relatively slow streamwise variation of the vortex motion. Also here, $y = \varepsilon^3 y'$ with y' of order unity.

So the main TS wave is governed by the linear inviscid system

$$u_X^{(1)} + v_{y'}^{(1)} + w_Z^{(1)} = 0,\ u_X^{(1)} = -p_X^{(1)}, v_X^{(1)} = -p_{y'}^{(1)},\ w_X^{(1)} = -p_Z^{(1)}, \tag{4.2}$$

$$p^{(1)} \to \bar{p}^{(1)},\ p_{y'}^{(1)} \to \alpha^2(A_{11}E_1 + A_{12}E_2) + c.c. \text{ as } y' \to 0+ \tag{4.3a,b}$$

and with suitable boundedness conditions in the farfield. The constraints (4.3a,b) match the pressure and normal velocity with those in the main deck of Section 2, thus ensuring the matching of the streamwise and spanwise velocities as well. A decomposition as in (2.4) applied to $p^{(1)}$ then produces the pressure-displacement law anticipated in (3.12f), since $p^{(1)}$ satisfies Laplace's equation, from (4.2).

In similar vein, the forced TS contribution satisfies in effect a forced version of the system (4.2) - (4.3) and that leads to the law quoted already in (3.15). The induced vortex flow, on the other hand, is governed by the effective cross-flow balances

$$v_{y'}^{(3)} + w_Z^{(3)} = 0,\ v_X^{(3)} = -p_{y'}^{(3)},\ w_X^{(3)} = -p_Z^{(3)} \tag{4.4}$$

here because of its comparatively small u, p parts, and the streamwise balance $u\frac{(3)}{X} = -p\frac{(3)}{X}$ is subsidiary. Hence under decomposition, and merging with the main-deck pressure,

$$p^{(3)} = \overline{p}_{33} \exp(-\beta y') E_3 + c.c. \tag{4.5}$$

and the displacement-or v-match then gives the result

$$\beta \overline{p}_{33} = -A_{33\overline{X}\,\overline{X}}. \tag{4.6}$$

This fixes the vortex pressure $\overline{p}_{33}(\overline{X})$ in the boundary layer in terms of the displacement $-A_{33}$ which is to be determined by the buffer-vortex problem (3.5). We observe that the induced pressure $\varepsilon^6 p^{(3)}$ above has relatively little feedback effect on the properties holding inside the boundary layer. Thus, the induced vortex's effects on the TS waves, during the present regime, are confined predominantly within the boundary layer (and, further, within the buffer and lower decks), even though the actual vortex motion produced spreads significantly far outside the boundary layer into the upper deck. See also Fig. 1.

The upper-deck vortex pattern also produces nonzero slip-velocity components $u^{(3)}, w^{(3)}$ at the upper edge of the main deck, as $y' \to 0+$. These induced slip velocities tie in with the expressions proposed previously for the main, buffer and lower decks, e.g., see the term $\overline{w}_{3E}$ in (2.2), but, like the induced vortex pressure above, they play no role in the dominant nonlinear interaction between the TS wave and its induced vortex. This TS-vortex nonlinear interaction is addressed further in the following section.

5. THE NONLINEAR INTERACTION EQUATIONS, AND SOLUTION PROPERTIES

In summary, the nonlinear induced vortex/TS interaction requires us to solve the following nonlinear partial-ordinary differential system consisting of three parts: first,

$$\begin{cases} U_{\overline{X}} + V_{\hat{y}} + i\beta W = 0, \\ \hat{y} U_{\overline{X}} + V = U_{\hat{y}\hat{y}}, \\ \hat{y} W_{\overline{X}} + iK|P|^2 \hat{y}^{-2} = W_{\hat{y}\hat{y}}, \end{cases} \tag{5.1a-c}$$

$$\begin{cases} U \to 0,\ V \to 0,\ W \sim -iK|P|^2 \ell n \hat{y} + \Phi(\overline{X}),\ \text{as } \hat{y} \to 0, \\ U \to A,\ V \sim -A\hat{y},\ W \propto \hat{y}^{-3},\ \text{as } \hat{y} \to \infty \end{cases} \tag{5.1d,e}$$

for the vortex (U, V, W); second,

$$P_{\overline{X}} + (c_1 \lambda_b \overline{X} + c_2 \lambda_{33}) P = 0 \tag{5.2a}$$

for the TS amplitude (P), where

$$\lambda_{33}(\overline{X}) \equiv U_{\hat{y}}(\overline{X},0); \tag{5.2b}$$

and, third, using the expression (3.18a),

$$\int_0^Y \{\int_\infty^{Y_2} \tilde{w}''_{33}(\overline{X},Y_1)dY_1\}dY_2 \sim -iK|P|^2 \ell nY + \Phi(\overline{X}), \tag{5.3a}$$

$$\Rightarrow \Phi(\overline{X}) = |P|^2\phi \tag{5.3b}$$

for the determination of the constant ϕ, and hence the function Φ, for a given spanwise wavenumber β. Here U, V, W, P, A can be related back to $\hat{u}_{33}, \hat{v}_{33}, \hat{w}_{33}, \overline{p}_{11}$ (or $\overline{p}_{12}$), A_{33}, although to fix matters we are focusing attention now on the case where $\overline{p}_{11} = \overline{p}_{12}$ and λ_{33} is real. Also,

$$K = \beta(1 - \beta^2/4\alpha^2), \tag{5.4}$$

while the constants $c_1 \equiv b/a$, $c_2 \equiv c/\lambda a$ in (5.2a) follow from evaluation of a, b, c in (3.17) for given β, and likewise for α from (3.14). The solution properties are addressed below, although most often with the $U - V - W$ formulation in (5.1) replaced by a $\tau - W$ formulation where W is still to be derived from (5.1c-e) but

$$\tau_{\hat{y}\hat{y}} - \hat{y}\tau_{\overline{X}} = -i\beta W, \tag{5.5a}$$

$$\tau \to 0 \text{ as } \hat{y} \to \infty, \ \tau_{\hat{y}} = 0 \text{ at } \hat{y} = 0 \tag{5.5b}$$

is then used to find $\tau(\equiv U_{\hat{y}})$ and hence

$$\lambda_{33}(\overline{X}) \equiv \tau(\overline{X},0). \tag{5.5c}$$

Here (5.5a,b) follow from (5.1a,b,d,e) and U, V, τ are real whereas W is pure imaginary.

Computational solutions of the interactive problem in question, (5.1c-e) with (5.2a), (5.3), (5.5), were sought with a simple implicit finite-difference procedure marching forward in $\overline{X}$, for several spanwise wavenumbers β defining K in (5.4), as follows. Given the solution up to the station $\overline{X} = \overline{X}_{n-1}$ say, the W profile at the next station $\overline{X}_n = \overline{X}_{n-1} + \Delta\overline{X}$ is obtained by inversion of the tridiagonal system

$$(W^A_{nj+1} - 2W^A_{nj} + W^A_{nj-1})/\Delta\hat{y}^2 - \hat{y}_j(W^A_{nj} - W^A_{n-1j})/\Delta\overline{X} = -\gamma_1\hat{y}_j\ell n(\hat{y}_j), \ j = 2 \to J-1, \tag{5.6a}$$

$$W^A_{n1} = \phi|P_{n-1}|^2, \tag{5.6b}$$

$$W^A_{nJ} = +\gamma_0\ell n(\hat{y}_J) \tag{5.6c}$$

representing (5.1c-e), after the substitution $W = -\gamma_0\ell n\hat{y} + W^A$ to keep W^A finite at $\hat{y} = 0$. Here $\Delta\overline{X}, \Delta\hat{y}$ are suitably small grid sizes, the subscripts n, j denote the function values

at the gridpoints $\overline{X}_n, \hat{y}_j[\equiv (j-1)\Delta\hat{y}$ for $j = 1$ to $J], \gamma_0 \equiv +iK|P|^2, \hat{y}_J$ is a suitably large edge value of $\hat{y}$, and $\gamma_0, \gamma_1[\equiv d\gamma_0/d\overline{X}]$ in (5.6a,c) are evaluated from the known previous solution values, as with $|P_{n-1}|^2$ in (5.6b). Also, the number ϕ is prescribed for a given β: see below. Next, the τ profile at $\overline{X}_n$ follows in a similar manner from inverting the tridiagonal form

$$(\tau_{nj+1} - 2\tau_{nj} + \tau_{nj-1})/\Delta\hat{y}^2 - \hat{y}_j(\tau_{nj} - \tau_{n-1j})/\Delta\overline{X} = -i\beta\{W^A_{nj} - \gamma_0 \ell n(\hat{y}_j)\} \ (j = 2 \rightarrow J-1), \tag{5.6d}$$

$$\tau_{n1} = \tau_{n2}, \tag{5.6e}$$

$$\tau_{nJ} = 0, \tag{5.6f}$$

associated with (5.5a,b), thus yielding the skin-friction factor (5.5c) as

$$(\lambda_{33})_n = \tau_{n1}. \tag{5.6g}$$

Finally at this station, P_n is found from an analogue of (5.2a),

$$P_n = P_{n-1} + \Delta\overline{X}[c_1\lambda_b\overline{X}_n + c_2(\lambda_{33})_n]P_{n-1}, \tag{5.6h}$$

and then the scheme (5.6a-h) can be moved on to the next station downstream, and so on. Many other numerical procedures suggest themselves of course, but the above procedure proved to be stable and accurate for sufficiently small step sizes: see also Figures 2-5 where sample interaction results are presented, all starting at position $\overline{X} = -1$ upstream of the neutral TS point.

The results shown are for the specific cases $\beta = 1, 1.6, 2, 2.5$ [see reasons later], for which the constants involved in the nonlinear interaction equations are as follows (see also Figure 1(b)):

β	α	θ	a	b	c	ϕ
1	0.904	28.85°	-1.09 - 2.84i	-0.59 - 0.99i	-0.56 - 0.49i	12.32i
1.6	0.754	46.70°	-1.59 - 3.66i	-0.83 - 1.20i	-0.70 + 0.17i	63.6i
2	0.617	58.32°	-2.53 - 5.24i	-1.09 - 1.57i	-0.84 + 0.88i	179.3i
2.5	0.433	70.89°	-5.79 - 10.78i	-1.75 - 2.51i	-1.25 + 2.32i	679i

The normalized case $\lambda = 1, \lambda_b = -1$ is assumed here, while the a, b, c values follow from numerical evaluation of (3.17), α from (3.14) and ϕ comes from (3.18) - (3.19) (or (5.3)) after some extensive grid-effect studies to allow for the rather slow approach to the asymptote there. We observe that since λ_{33} is real P could be replaced by $|P|$ in (5.2a) with c_{1r}, c_{2r} then replacing c_1, c_2 respectively. Also in the table above θ gives the TS wave angles $\tan^{-1}(\beta/2\alpha)$.

The ultimate behavior of the nonlinear interactive flow, as $\overline{X}$ increases, is considered analytically now. There appear to be several possible options, the first of which has an algebraic singularity arising at a finite position, say as $\overline{X} \to \overline{X}_0-$. The orders of magnitude suggest the balances $\tau \sim \lambda_{33} \sim |\partial_{\overline{X}}|$, from (5.2a), (5.5c), $|\partial_{\hat{y}}|^3 \sim |\partial_{\overline{X}}|$ and $W \sim |\partial_{\overline{X}}|^{\frac{5}{3}}$ from (5.5a), and hence $P \sim |\partial_{\overline{X}}|^{\frac{5}{6}}$, approximately, from (5.1c,d), (5.3). So, with allowance for the logarithmic term in (5.1d), the proposed local response as $\overline{X} \to \overline{X}_0-$ is of the form

$$|P| \sim (\overline{X}_0 - \overline{X})^{-\frac{5}{6}} L^{-\frac{1}{2}} |\tilde{P}|, \; W \sim (\overline{X}_0 - \overline{X})^{-\frac{5}{3}} \tilde{W}, \tag{5.7a,b}$$

$$(\tau, \lambda_{33}) \sim (\overline{X}_o - \overline{X})^{-1} (\tilde{\tau}, \tilde{\lambda}_{33}), \; \eta \equiv \hat{y} (\overline{X}_0 - \overline{X})^{-\frac{1}{3}}, \tag{5.7c,d}$$

to leading order, with $L \equiv -\ell n(\overline{X}_0 - \overline{X})$ and $\tilde{P}, \tilde{\lambda}_{33}$ unknown constants. Here the vortex system reduces to the ordinary differential equations for $\tilde{W}(\eta), \tilde{\tau}(\eta)$,

$$\tilde{W}'' - \eta^2 \tilde{W}'/3 - 5\eta \tilde{W}/3 = 0 \tag{5.8a}$$

$$\tilde{\tau}'' - \eta^2 \tilde{\tau}'/3 - \eta \tilde{\tau} = -i\beta \tilde{W} \tag{5.8b}$$

subject to

$$\tilde{W}(\infty) = \tilde{\tau}(\infty) = \tilde{\tau}'(0) = 0, \; \tilde{W}(0) = iK|\tilde{P}|^2/3 \tag{5.8c-f}$$

and the TS part requires, for consistency,

$$\frac{5}{6} = -c_{2r} \tilde{\lambda}_{33} \tag{5.9}$$

where $\tilde{\lambda}_{33} = \tilde{\tau}(0)$. It is worth noting that here and in the subsequent option the TS forcing on the vortex makes itself felt only through a constant inner constraint on $\tilde{W}$, here (5.8f), which is due to the logarithmic contribution in (5.1d), the other forcings [$\propto K$ in (5.1c) and ϕ in (5.1d)] being negligible at this level, as is the linear-growth term $\propto c_1$ in this case. The solution for $\tilde{W}$ as a function of $\sigma \equiv \eta^3$ is

$$\tilde{W}(\sigma) = K_1 \int_0^\infty r^{\frac{2}{3}} (r + \frac{1}{9})^{-2} e^{-r\sigma} dr, \; K_1 \equiv iK|\tilde{P}|^2 / \{3^{\frac{5}{3}} \Gamma(\frac{1}{3}) \Gamma(\frac{5}{3})\} \tag{5.10a}$$

and therefore

$$\tilde{\tau}(\sigma) = \sigma^{\frac{1}{3}} e^{\sigma/9} \int_\infty^\sigma s_1^{-\frac{4}{3}} e^{-s_1/9} \{-i\beta \int_\infty^{s_1} \tilde{W}(s_2) s_2^{-\frac{1}{3}} ds_2 + \tilde{B}\} ds_1/9 \tag{5.10b}$$

with $\tilde{B}$ chosen to make $d\tilde{\tau}/d\eta$ zero at $\sigma = 0$, from (5.8a-f). This then gives $\tilde{\lambda}_{33} = -[i\beta \int_0^\infty \tilde{W}(s_2) s_2^{-\frac{1}{3}} ds_2 + \tilde{B}]/3$. Hence the existence of this local algebraic break-up depends on the relation

$$c_{2r} K |\tilde{P}|^2 = d_3 \tag{5.11}$$

being satisfied, because of (5.9). Here d_3 is a positive real constant. Since $|\tilde{P}|^2$ is to be positive, the break-up (5.7) is therefore a candidate for the ultimate interaction behavior in the regime where $c_{2r}K$ is positive. This regime covers all wave angles θ except for a small interval of θ between 45° and approximately 50° where Kc_{2r} goes negative, as shown in Fig. 1(b).

The second option, in contrast, has the solution continuing to downstream infinity, where an algebraic response takes effect, namely

$$|P| \sim \overline{X}^{\frac{1}{6}} L^{-\frac{1}{2}} |\tilde{P}|, \; W \sim \overline{X}^{\frac{1}{3}} \tilde{W}(\eta), \tag{5.12a,b}$$

$$(\tau, \lambda_{33}) \sim \overline{X}(\tilde{\tau}, \tilde{\lambda}_{33}), \; \eta \equiv \hat{y}\overline{X}^{-\frac{1}{3}}, \tag{5.12c,d}$$

as $\overline{X} \to \infty$, with $L \equiv \ell n \overline{X}$ now. This option arises from balancing the growth terms $\propto c_1, c_2$ in (5.2a), yielding (5.12c), then (5.12b,d) follow from (5.5a), after which (5.1d) suggests the size in (5.12a). Thus here the $\overline{X}$-derivative in (5.2a) and the forcing terms $\propto K, \Phi$ in (5.1c,d) are negligible to leading order. The controlling equations and conditions for this option are

$$\tilde{W}'' + \eta^2 \tilde{W}'/3 - \eta \tilde{W}/3 = 0, \tag{5.13a}$$

$$\tilde{\tau}'' + \eta^2 \tilde{\tau}'/3 - \eta \tilde{\tau} = -i\beta \tilde{W}, \tag{5.13b}$$

$$\tilde{W}(\infty) = \tilde{\tau}(\infty) = \tilde{\tau}'(0) = 0, \; \tilde{W}(0) = -iK|\tilde{P}|^2/3. \tag{5.13c}$$

$$0 = c_{1r}\lambda_b + c_{2r}\tilde{\lambda}_{33}, \text{ where } \tilde{\lambda}_{33} = \tilde{\tau}(o), \tag{5.13d}$$

from substitution of (5.12) into (5.1)-(5.5), and so we have the solutions

$$\tilde{W} = i(K|\tilde{P}|^2/3)\eta \int_{\infty}^{\eta} \eta_1^{-2} \exp(-\eta_1^3/9) d\eta_1, \tag{5.14a}$$

$$\tilde{\tau} = \beta(K|\tilde{P}|^2/27) \int_{\sigma}^{\infty} \int_{s_2}^{\infty} s_1^{-\frac{4}{3}} \exp(-s_1/9) ds_1 ds_2. \tag{5.14b}$$

Here $\sigma = \eta^3$. Therefore $\tilde{\lambda}_{33} = \beta(K|\tilde{P}|^2/9)\Gamma(2/3)3^{\frac{1}{3}}$, from (5.14b), and (5.13d) then gives the relation

$$\beta|\tilde{P}|^2 c_{2r} K = d_4 \tag{5.15}$$

where, since $\lambda_b = -1$ and c_{1r} is always positive, the constant d_4 is positive. In consequence this option 2 also applies for positive values of Kc_{2r} only.

Option 3 is that the nonlinear solution amplifies exponentially as $\overline{X} \to \infty$, with a growth $\exp(s\overline{X}/2)$, say, in $|P|$ forcing a vortex flow of amplitude $\exp(s\overline{X})$ (from 5.1c,d)) which in turn requires the c_2 term in (5.2a) to dominate alone. Thus

$$|P| \sim \exp(s\overline{X}/2)|\tilde{P}|, \; W \sim \exp(s\overline{X})\tilde{W}, \tag{5.16a,b}$$

$$(\tau, \lambda_{33}) \sim \exp(s\overline{X})(\tilde{\tau}, \tilde{\lambda}_{33}),\ \hat{y} \sim 1. \qquad (5.16c,d)$$

Then from (5.1)-(5.5) the leading balances are

$$\begin{cases} \tilde{W}'' - s\hat{y}\tilde{W} = iK|\tilde{P}|^2\hat{y}^{-2}, \\ \tilde{\tau}'' - s\hat{y}\tilde{\tau} = -i\beta\tilde{W} \end{cases} \qquad (5.17a,b)$$

with

$$\tilde{W}(\infty) = \tilde{\tau}(\infty) = \tilde{\tau}'(0) = 0, \tilde{W} \sim |\tilde{P}|^2\{-iK\ell n\hat{y} + \phi\} \text{ as } \hat{y} \to 0 \qquad (5.17c-f)$$

and

$$\tilde{\lambda}_{33} = \tilde{\tau}(0) = 0. \qquad (5.18)$$

The positive constant s is to be determined. The solution of (5.17) can be expressed as

$$\tilde{W} = iK|\tilde{P}|^2 M(\tilde{y}),\ \tilde{\tau} = s^{-\frac{2}{3}}\beta K|\tilde{P}|^2 N(\tilde{y}),\ \tilde{y} = s^{\frac{1}{3}}\hat{y} \qquad (5.19a)$$

with

$$M(\tilde{y}) = B_1 Ai(\tilde{y}) - \ell n\tilde{y} - Ai(\tilde{y})\int_0^{\tilde{y}} Ai^{-2}(y_1)\{\int_\infty^{y_1} y_2 Ai(y_2)\ell n y_2 dy_2\}dy_1, \qquad (5.19b)$$

$$N(\tilde{y}) = B_2 Ai(\tilde{y}) + M'(\tilde{y}) + \tilde{y}^{-1} + Ai(\tilde{y})\int_0^{\tilde{y}} Ai^{-2}(y_1)\{\int_\infty^{y_1} Ai(y_2)dy_2\}dy_1 \qquad (5.19c)$$

where Ai is the Airy function again and $B_1 Ai(0) = (\ell ns)/3 - i\phi/K, B_2 Ai'(0) = 1/(3Ai(0))$. Hence $\tilde{\lambda}_{33} \propto N(0)$ follows, and the requirement (5.18) leads to the real positive value

$$s = \exp(-e_1/e_2) \qquad (5.20)$$

for the growth factor s, where $e_1 = 1.21 - 0.73i\phi/K, e_2 = 0.243$. This option, in which (unlike in options 1,2) all the TS forcings on the vortex flow play a substantial part, is therefore a versatile one in the sense that it is available for all values of K, c_{1r}, c_{2r}, i.e., for all wave angles.

Option 4 has the TS disturbance $|P|$ becoming very small/negligible, and the vortex flow then grows slowly on its own with distance $\overline{X}$, from its initial state upstream. This option is ultimately unstable to the TS waves (if present) however, via (5.2a), since the vortex skin friction λ_{33} is insufficient to counteract the nonparallel-growth term $\propto \lambda_b$ downstream.

The computations described earlier tend to support option 1 in the cases where Kc_{2r} is positive, i.e. for the spanwise wavenumbers $\beta = 1, 2, 2.5$, although the finite-distance break-up associated with that option can be delayed for a very long distance, depending

on the starting conditions upstream: see the figures. It is interesting that the long delay corresponds in fact to the near-attainment of option 4. For the case $\beta = 1.6$, in contrast, where Kc_{2r} is negative, the computations seem to point to the long-scale exponential option 3 being approached downstream, the rapid growth in that case being ascribed to the enormous nonlinear growth factor $s \approx 10^{410.7}$ from (5.20), which in turn is due mostly to the numerical largeness of $|\phi/K|$ when $\beta = 1.6$. The value of s is also large for the other spanwise wavenumbers although there the option 1 appears to take preference, as might be expected. The relevance of all these options (and we note that no others have been found yet) is discussed in the next section.

6. FURTHER DISCUSSION

Two immediate extensions of the theory should be mentioned first and they concern external pressure gradient effects and unequal TS amplitudes, respectively. The influence of an external pressure gradient or non-uniform slip velocity just outside the boundary layer is accommodated by the present nonparallel-flow theory through the term involving c_1 in (5.2a), which in turn comes from the normalized TS dispersion relation (3.13) in effect. In dimensional variables (denoted by "D") this shows that the frequency Ω_D is related to the triple-deck frequency, Ω_{TD} say, by $\Omega_D = (\partial u_D/\partial y_D)_w^{\frac{3}{2}} \Omega_{TD} u_\infty \nu_\infty^{\frac{1}{2}} (u_D)_e^{-2}$ locally, where w stands for the dimensional value at the wall and ∞ for the dimensional reference value, e.g., far upstream, while $(u_D)_e$ is the external slip velocity. For a fixed input frequency Ω_D upstream (and fixed $u_\infty, \ell_\infty, \nu_\infty$), therefore, Ω_{TD} increases or decreases, i.e. the TS waves are destabilized or stabilized (corresponding to $\lambda_b = \mp 1$ in effect), according as the combination $(\partial u_D/\partial y_D)_w^{\frac{3}{2}} (u_D)_e^{-2}$ decreases or increases, in turn. Thus the issue depends on the basic boundary-layer slip velocity and the wall shear. For instance, a favorable pressure gradient has $(u_D)_e$ increasing but that then tends to increase the wall shear also, so reducing the stabilizing trend. A sufficiently favorable presure gradient could lead to an effective change in the sign of λ_b, nevertheless, in (5.2a), and that then alters the nonlinear interaction properties, as indeed the options 1-4 in Section 5 would suggest. An example of a computation associated with the stabilizing value $\lambda_b = 1$ is shown in Figure 6. Next, the special case of equal TS pressures $\overline{p}_{11}, \overline{p}_{12}$, taken in Section 5, holds also for the broader case where $|\overline{p}_{11}|, |\overline{p}_{12}|$ are equal with the phases of $\overline{p}_{11}, \overline{p}_{12}$ differing, i.e. the phase difference is insignificant then. The most general case of unequal $|\overline{p}_{11}|, |\overline{p}_{12}|$ however is not covered yet. It might be argued that the options 1-4 describe the ultimate response even in the most general case but the effects of unequal amplitudes and the associated rise in significance of the phases remain to be seen. The special case of 45° waves where the interaction constant K is zero may require more research as well.

Comparisons between the present study and corresponding experiments as well as previous computational work tend to be favorable on the qualitative features, if not more. This is particularly so with respect to the implied abrupt break-up or change in scale of the streamwise vortex motion (in option 1), due to the generation of the oblique TS waves and then nonlinear interaction. A number of other features (e.g., see scales below) also seem common to the theory and the experiments.

The present approach is based on a rational scheme throughout, we should stress, which is aimed among other things at shedding light on the scales which are central to TS/vortex interaction and hence to transition. The scales of the pressure and velocity disturbance levels associated with the current nonlinear-interaction regime for instance are quite small, as (2.2), (3.1), (3.7), (4.1) show; e.g., the streamwise velocity disturbance implied in (4.1) is approximately 0.4% of the free stream velocity at a global Reynolds number of 10^6. The theory also accounts for nonparallel-flow effects in a rational way, which is a vital aspect in the boundary-layer context, and as yet there appears to be no alternative acceptable theoretical approach.

Addressing the further implications of the theory, we feel that the main repercussions stem from the options 1-4 for the terminal behavior of the nonlinear TS/induced-vortex interaction described at the end of the previous section. See the sketch in Figure 7. Option 1 indicates a shortening of the streamwise interaction scale, as the break-up in (5.7) takes place, together with enhanced vortex and TS amplitudes. In fact, when $\overline{X}_0 - \overline{X}$ shortens to $0(\varepsilon^{\frac{3}{2}})$ the reduced pressure amplitude $|P|$ rises to $0(\varepsilon^{-\frac{5}{4}})$, formally, apart from a logarithmic factor, thus forcing the unscaled wall pressure p (e.g., in (3.7)) to rise to $0(\varepsilon^2)$. Along with that, the scaled spanwise vortex velocity W increases to $0(\varepsilon^{-\frac{5}{2}})$, from (5.7), meaning that the un-scaled vortex w-contribution increases to $0(\varepsilon^{\frac{7}{2}}.\varepsilon^{-\frac{5}{2}})$, i.e. $0(\varepsilon)$, from (3.1) or (3.7), in the buffer or lower deck; and the typical buffer thickness $0(\varepsilon^{\frac{9}{2}}|\hat{y}|)$ becomes $0(\varepsilon^{\frac{9}{2}}.\varepsilon^{\frac{1}{2}})$, i.e., $0(\varepsilon^5)$, coincident with the lower-deck thickness. All these scales, and the others present, imply that the next stage encountered beyond the break-up in (5.7) brings in the fully nonlinear unsteady 3D triple-deck response on the $0(\varepsilon^3)$ length scale (streamwise and spanwise), that is, the 3D unsteady boundary-layer equations with pressure-displacement interaction. The 3D triple-deck description (see computations by Smith (1988)) then controls both the nonlinear TS and the induced-vortex behavior. An interpretation of the above is that the nonlinear 3D TS/vortex interaction addressed in the present work provides a powerful mechanism for small input disturbances upstream to "burst" abruptly through to full nonlinear-TS status, at a sub- or super-critical location, via the singular behavior in (5.7).

Option 2, on the other hand, has the streamwise scale lengthening downstream as

indicated in (5.12). Indeed, when the typical un-scaled distance x enlarges to the airfoil scale 0(1), i.e. $\overline{X} \rightarrow 0(\varepsilon^{-\frac{3}{2}})$ formally, then the vortex skin-friction factor λ_{33} rises to $0(\varepsilon^{-\frac{3}{2}})$, from (5.12), suggesting an increased contribution of order ε in the lower-deck velocity u in (3.7a). This is comparable with the basic-flow contribution $(\varepsilon\lambda Y)$ there and so changes the TS stability characteristics. Simultaneously the buffer thickness $0(\varepsilon^{\frac{9}{2}}|\hat{y}|)$ rises to $0(\varepsilon^4)$, meaning that the main boundary layer is affected more substantially than before by the vortex flow, and the u-velocity component of the vortex rises to 0(1). Thus the entire boundary-layer flow is also altered, in the implied next stage. This long-scale next stage is examined by Hall and Smith (1988).

The subsequent or "second" stages inferred above, as well as the long-scale ones corresponding to options 3,4, clearly merit further study. This is partly to understand more the ensuing behavior in the TS/vortex interactions which start in the present regime (of (2.1)), of course, but partly also to tackle the interactions that can arise with higher input amplitudes leading directly into those second stages, i.e. the by-pass process. That process makes all the second stages available in effect, provided the latter are self-consistent as in options 1-4, even if they cannot be reached via the smaller-amplitude first stage.

Another aspect worthy of further investigation corresponds to taking the spanwise wavenumber β small, to study the 3D de-stabilization of an incident 2D nonlinear TS wave. The scales in the present regime provide a starting point for such an investigation, including the influence of nonparallelism. The theoretical approach is believed to apply to a number of other interesting flow configurations as well, and to have a strong connection with some observed transition phenomena such as the creation of "Lambda vortices."

Finally, the importance of nonparallel-flow effects in certain interaction cases is re-emphasized. Some remarks on them have been made already in this section. Nonparallelism of the boundary layer is vital in both of the options 2,3, corresponding to long-scale induced vortex flow, and hence also in the second stages subsequent to those options. Neglect of the nonparallelism seems acceptable for the shortening interaction of option 1 and the like but it would lead to erroneous results otherwise.

ACKNOWLEDGEMENT

Comments by Mr. N. D. Blackaby and Mr. A. G. Walton are gratefully acknowledged.

References

[1] Antar, B. N. and Collins, F. G., 1975, Phys. Fluids **18**, 289.

[2] Aihara, Y., 1965, Bulletin Aero. Res. Inst., Tokyo Univ. **3**, 195.

[3] Aihara, Y. and Tani, I., 1969, J. Appl. Math. Phys. **20**, 609.

[4] Aihara, Y. and Koyama, H., 1981, Trans. Jap. Soc. Aero. Space Sci. **24**, 78-94.

[5] Aihara, Y., Tomita, Y., and Ito, A., 1985, in "Laminar-Turbulent Transition," 447-454, V. V. Kozlov (ed.), Springer-Verlag.

[6] Bennett, J., Hall, P., and Smith, F. T., 1988, ICASE Rept. 88-45.

[7] Benney, D. J. and Lin, C. C., 1960, Phys. Fluids **3**, 656.

[8] Bippes, H. and Görtler, H., 1972, Acta Mech. **14**, 251.

[9] Bushnell, D., 1984, A.I.A.A. paper presented at AIAA meeting, Snowmass, Colorado, June 1984.

[10] Hall, P., 1982, I.M.A. Jnl. Appl. Math. **29**, 173.

[11] Hall, P., 1988, J. Fluid Mech., in press.

[12] Hall, P. and Smith, F. T., 1984, Stud. in Applied Math. **70**, 91-120.

[13] Hall, P. and Smith, F. T., 1987, ICASE Rept. 87-25; also Proc. Roy. Soc., 1988, **A417**, 255-282.

[14] Klebanoff, P. S., Tidstrom, K. D., and Sargent, L. M., 1962, J. Fluid Mech. **12**, 1.

[15] Ryzhov, O. S. and Zhuk, V. I., 1986, in Current Problems in Computational Fluid Dynamics, p. 286. Moscow: MIR Publishers.

[16] Smith, F. T., 1979a, Proc. Roy. Soc. A **366**, 91-109.

[17] Smith, F. T., 1979b, Proc. Roy. Soc. A **368**, 573-589.

[18] Smith, F. T., Papageorgiou, D. T., and Elliott, J. W., 1984, J. Fluid Mech., **146**, 313-330.

[19] Smith, F. T. and Stewart, P. A., 1987, J. Fluid Mech. **179**, 227-252; see also Rept. UTRC86-26.

[20] Smith, F. T., 1988, Computers & Fluids, to appear; also R. T. Davis Memorial Symposium, Cincinnati, Ohio, presentation, June 1987.

[21] Spalart, P. R. and Yang, K.-S., 1986, NASA Tech. Memo. 88221.

[22] Srivastava, K. M. and Dallman, U., 1987, Phys. Fluids **30**, 1005-1015.

[23] Tani, I. and Sakagami, J., 1962, in "Procs. of the Int. Council on Aeron. Sci.," Third Congress, Stockholm, 391-403 (Spartan, New York).

[24] Wray, A. and Hussaini, M. Y., 1984, Proc. Roy. Soc. London **A392**, 373-389.

FIGURE CAPTIONS

Figure 1. (a) Diagram of the 3D TS/vortex structure for nonlinear interaction in a 2D boundary layer (BL): see also Fig. 7 below.

(b) Certain coefficients plotted against the TS wave angle θ.

Figure 2. Nonlinear-interaction computed results for $\beta = 1$, wave angle $\theta = 28.95°$. (a) Vortex shear λ_{33} vs. $\overline{X}$, (b) TS amplitude squared ($|P|^2$) vs. $\overline{X}$. Initial $|P| = 0.1$, initial vortex $[W, \tau] = [q_1\hat{y}, q_2(1+\hat{y}^2)]\exp(-\hat{y}^2)$. Case I: $(q_1, q_2) = (0,0)$. Case II: $(q_1, q_2) = (1,1)$. Grid has $(\Delta\overline{X}, J, \Delta\hat{y}) = (0.002, 801, 0.08)$ in general. Results $0, X$ are for grids (0.001, 801, 0.08), (0.001, 801, 0.04) in turn. Similar trends resulted for starting values $|P| = 1, 0.01, 0.001$.

Figure 3. Computed results for $\beta = 1.6$, wave angle $\theta = 46.70°$. Starting $|P| = 0.1$, with $(q_1, q_2) = (-5,-5), (1,1), (5,5)$ for cases I, II, III respectively. Grid (0.001, 1601, 0.08); doubling $\Delta\overline{X}, \Delta\hat{y}$ produced little change. Results for case (0,0) of starting vortex at rest are very close to those of case II.

Figure 4. Results for $\beta = 2$, wave angle $\theta = 58.32°$. Start $|P| = 0.1, (q_1, q_2) = (0,0)$; results for (1,1) are almost identical. Grid (0.001, 1601, 0.08).

Figure 5. Results for $\beta = 2.5$, wave angle $\theta = 70.89°$. Start $|P| = 0.1, (q_1, q_2) = (0,0)$; grid (0.002, 1601, 0.08). Results for starting $|P| = 0.1(\bullet)$ and for (1,1) (X) are also shown, as is typical effect (0) of doubling/halving $\Delta\overline{X}, J, \Delta\hat{y}$. Similar trends resulted for other starting conditions calculated.

Figure 6. Results for stabilizing case $\lambda_b = 1$.

Figure 7. Summary of (a) effect of wave angle of nonlinear breakdown and (b),(c) next higher-amplitude stages of short/long scale following breakdown options 1,2.

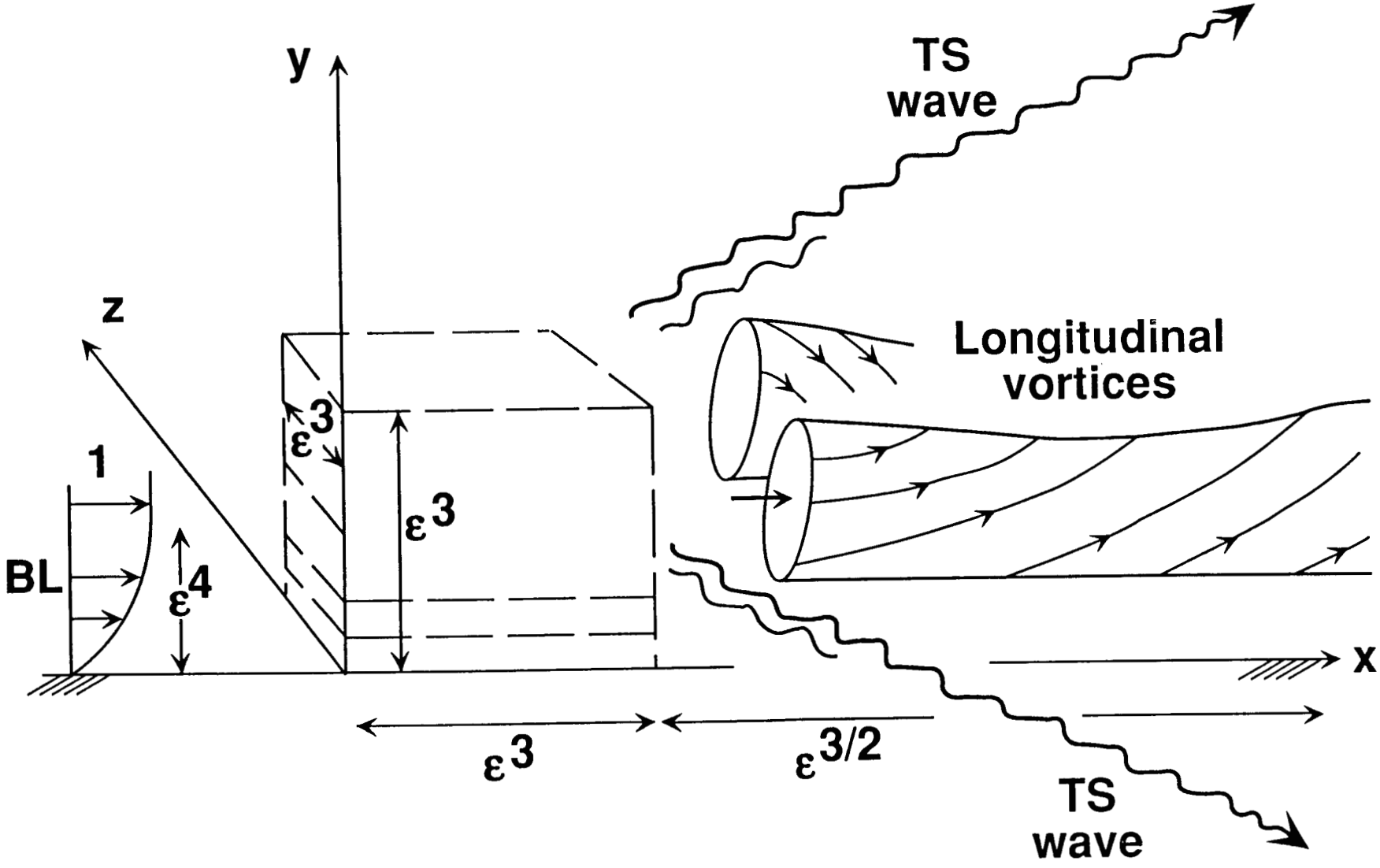

Fig. 1(a).

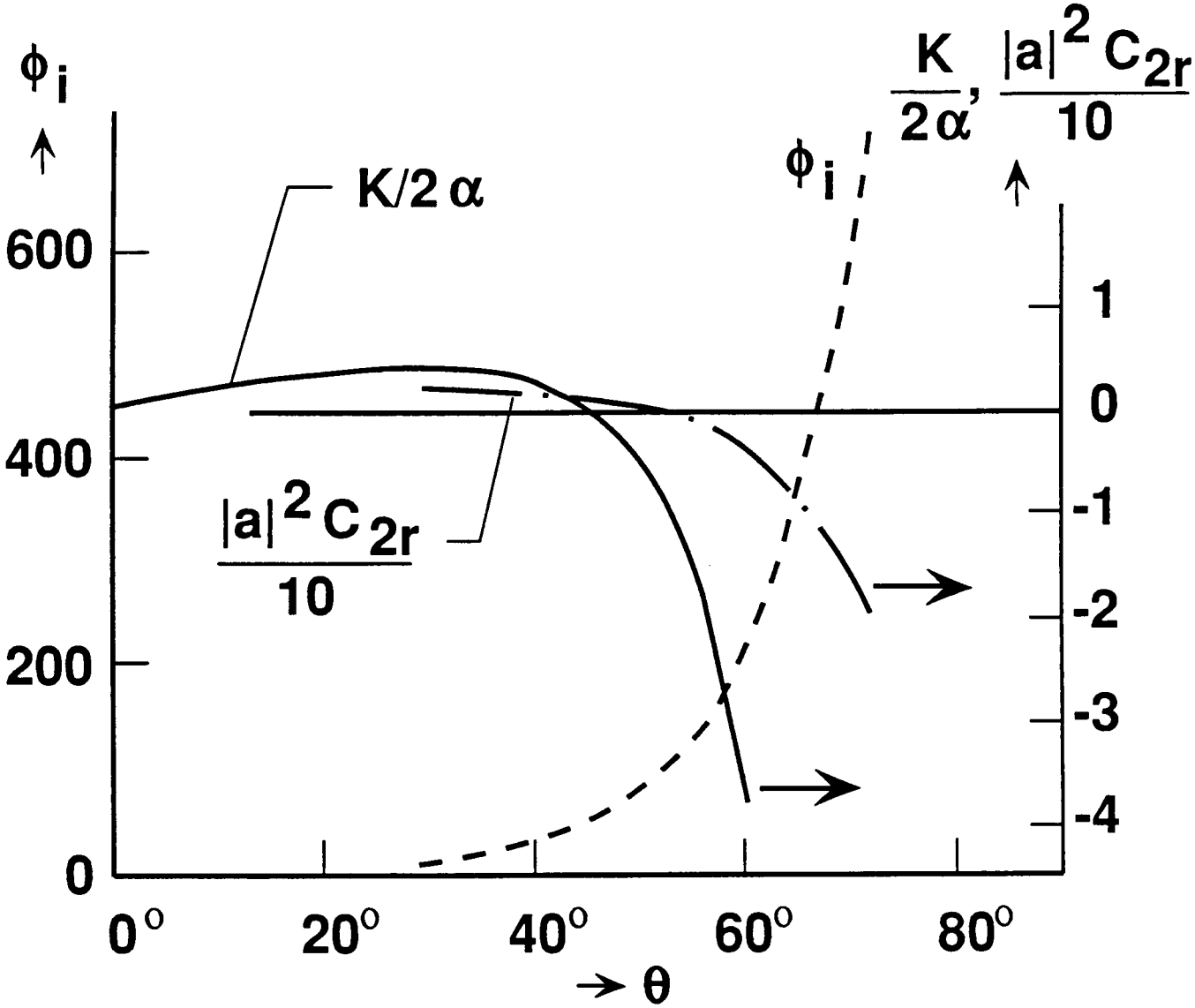
ϕ_i
$\frac{K}{2\alpha}, \frac{|a|^2 C_{2r}}{10}$
ϕ_i
$K/2\alpha$
$\frac{|a|^2 C_{2r}}{10}$
600
400
200
0
1
0
-1
-2
-3
-4
0°
20°
40°
60°
80°
θ

Fig. 1(b).

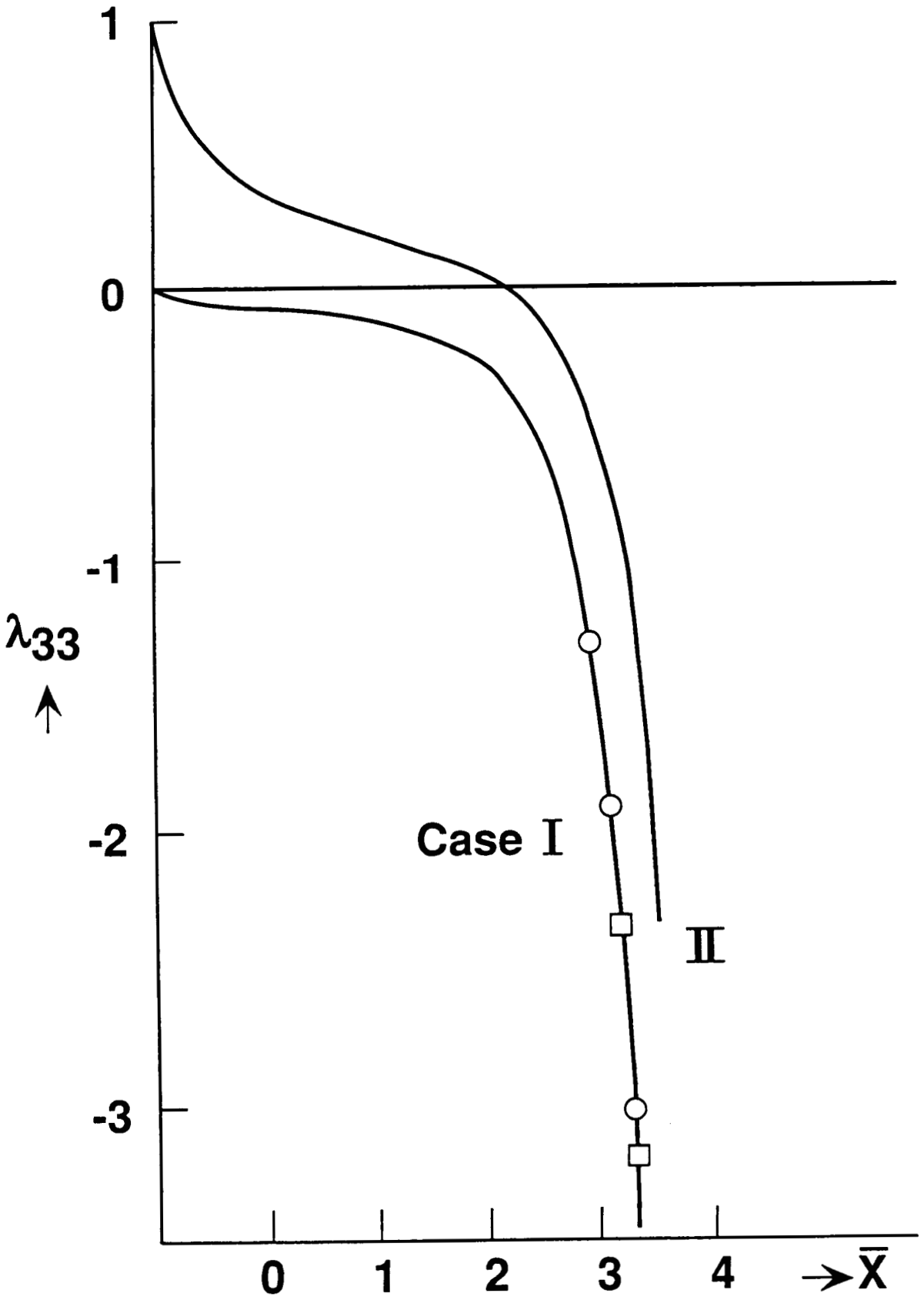

Fig. 2(a).

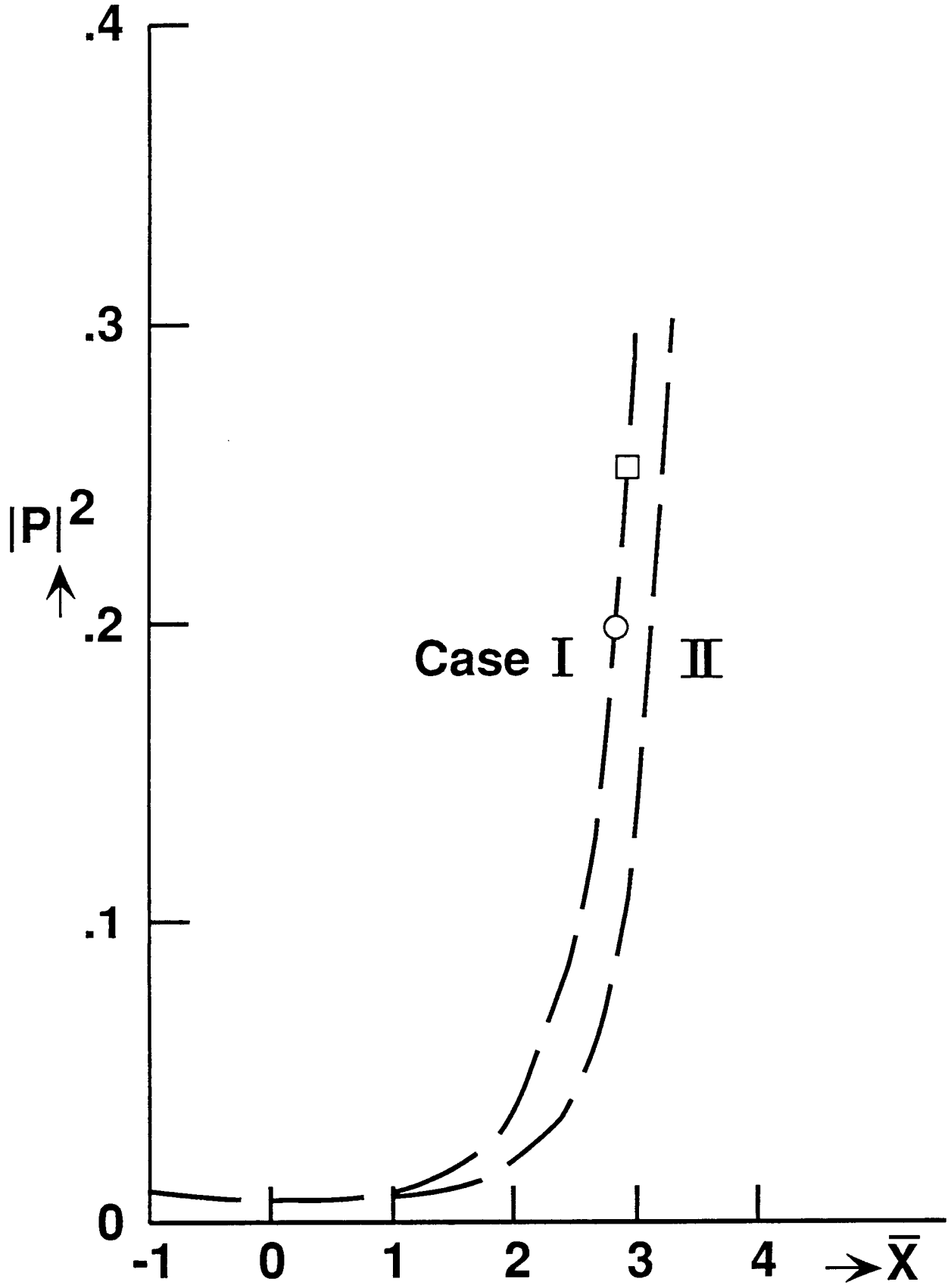

Fig. 2(b).

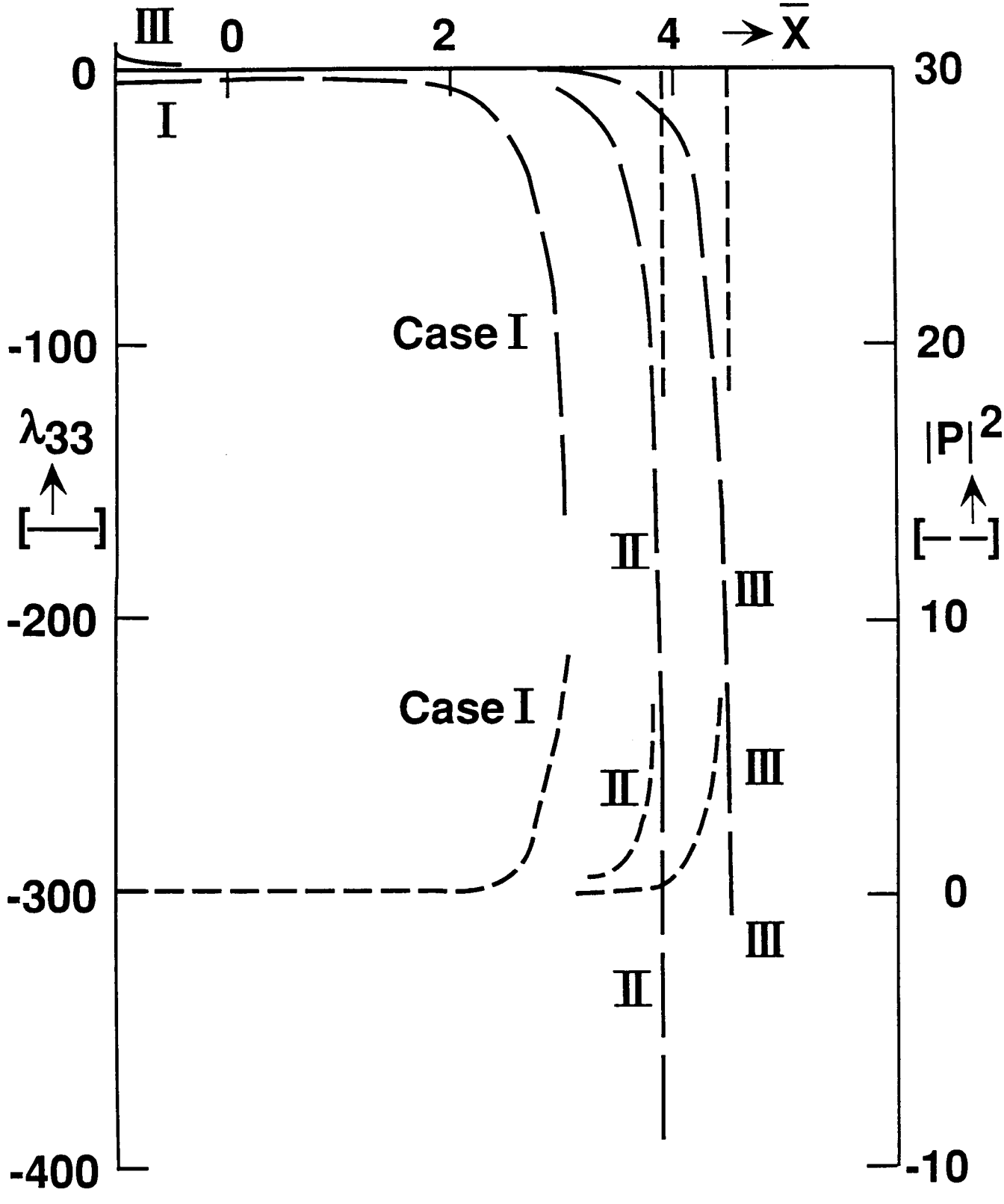
III
0
2
4
→X̄
0
30
I
-100
Case I
20
λ33
|P|2
[——]
[– –]
II
III
-200
10
Case I
II
III
-300
0
III
II
-400
-10

Fig. 3.

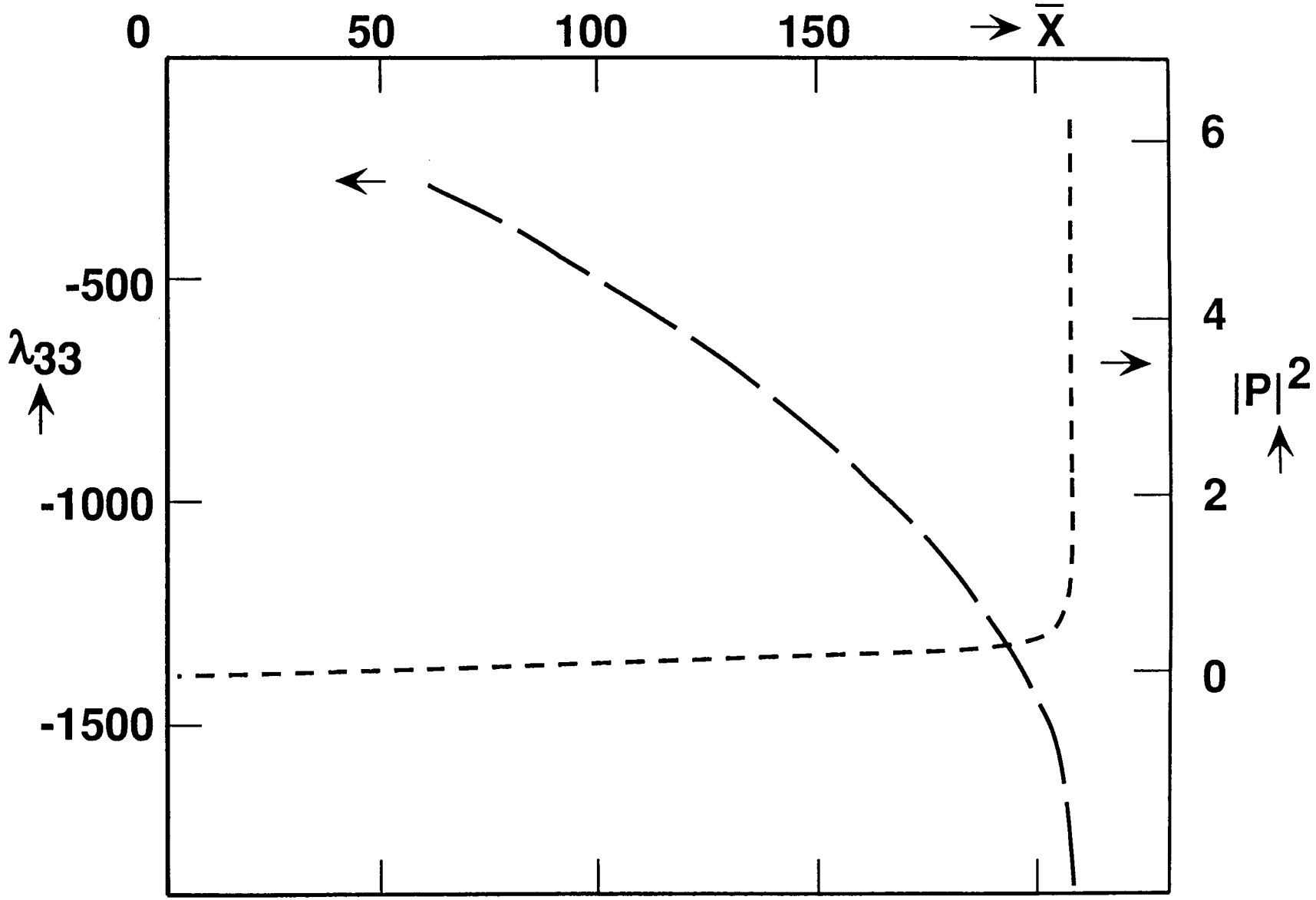

Fig. 4.

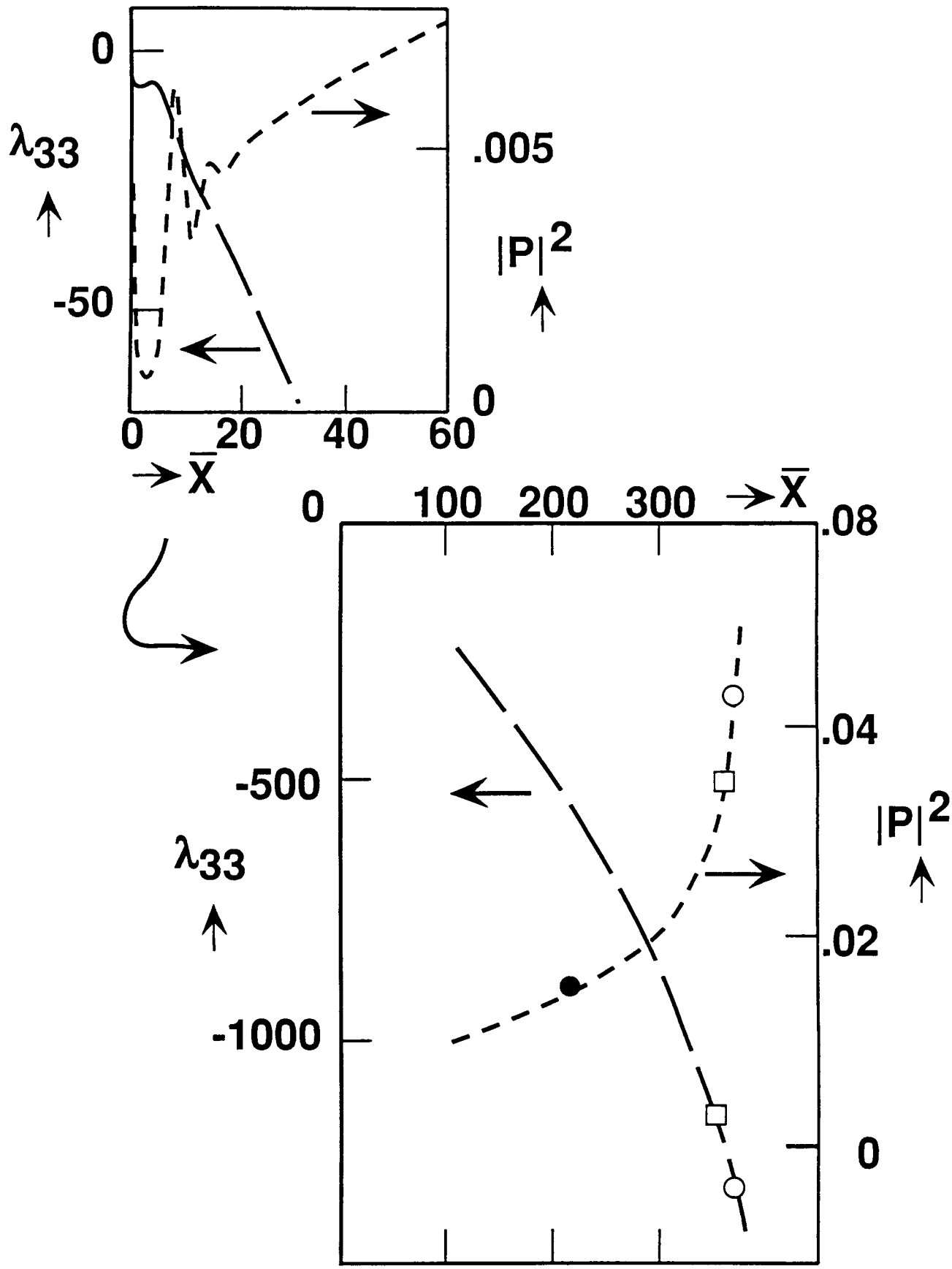
0
λ33
-50
.005
|P|2
0
0
20
40
60
X̄
0
100
200
300
X̄
.08
.04
-500
λ33
-1000
|P|2
.02
0

Fig. 5.

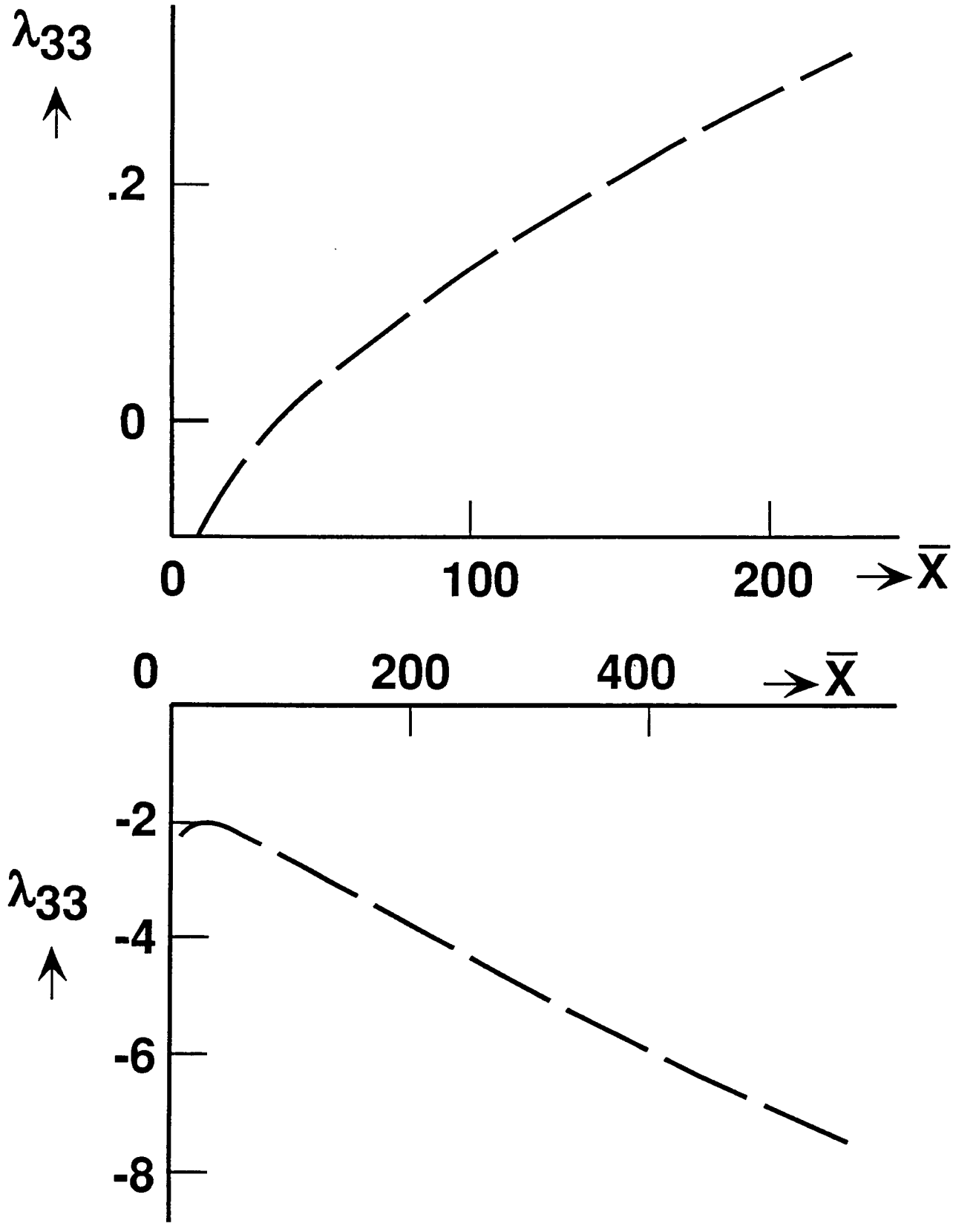

Fig. 6.

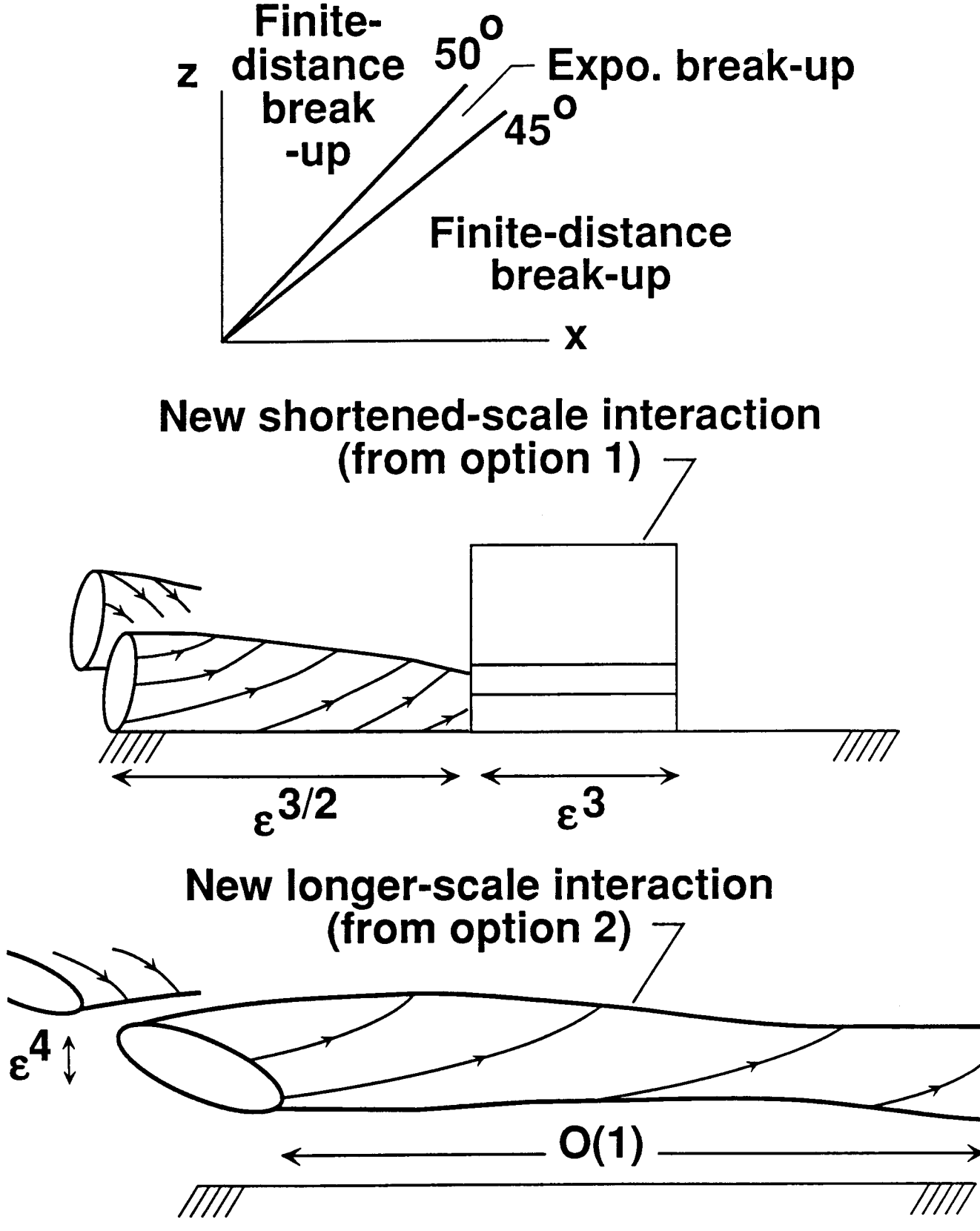
Finite-
distance
break
-up
z
50°
Expo. break-up
45°
Finite-distance
break-up
x
New shortened-scale interaction
(from option 1)
ε3/2
ε3
New longer-scale interaction
(from option 2)
ε4
O(1)

Fig. 7.

NASA
National Aeronautics and Space Administration

Report Documentation Page

1. Report No.	2. Government Accession No.	3. Recipient's Catalog No.
NASA CR-181698 ICASE Report No. 88-46		

4. Title and Subtitle	5. Report Date
NONLINEAR TOLLMIEN-SCHLICHTING/VORTEX INTERACTION IN BOUNDARY LAYERS	August 1988
	6. Performing Organization Code

7. Author(s)	8. Performing Organization Report No.
P. Hall and F. T. Smith	88-46
	10. Work Unit No. 505-90-21-01

9. Performing Organization Name and Address	11. Contract or Grant No.
Institute for Computer Applications in Science and Engineering Mail Stop 132C, NASA Langley Research Center Hampton, VA 23665-5225	NAS1-18107
	13. Type of Report and Period Covered Contractor Report
12. Sponsoring Agency Name and Address National Aeronautics and Space Administration Langley Research Center Hampton, VA 23665-5225	14. Sponsoring Agency Code

15. Supplementary Notes

Langley Technical Monitor:
Richard W. Barnwell

Submitted to Journal of Fluid Mechanics

Final Report

16. Abstract

The nonlinear interaction between two oblique three-dimensional Tollmien-Schlichting (TS) waves and their induced streamwise-vortex flow is considered theoretically for an incompressible boundary layer. The same theory applies to the de-stabilization of an incident vortex motion by sub-harmonic TS waves, followed by interaction. The scales and flow structure involved are addressed for high Reynolds numbers. The nonlinear interaction is powerful, starting at quite low amplitudes with a triple-deck structure for the TS waves but a large-scale structure for the induced vortex, after which strong nonlinear amplification occurs. This includes nonparallel-flow effects. The nonlinear interaction is governed by a partial-differential system for the vortex flow coupled with an ordinary-differential one for the TS pressure. The solution properties found sometimes produce a break-up within a finite distance and sometimes further downstream, depending on the input amplitudes upstream and on the wave angles, and that then leads on to the second stages of interaction associated with higher amplitudes, the main second stages giving either long-scale pheonomena significantly affected by nonparallelism or shorter quasi-parallel ones governed by the full nonlinear triple-deck response. Qualitative comparisons with experiments are noted.

17. Key Words (Suggested by Author(s))	18. Distribution Statement
transition, boundary layers, wave and vortex	01 - Aeronautics (General) 02 - Aerodynamics Unclassified - unlimited

19. Security Classif. (of this report)	20. Security Classif. (of this page)	21. No. of pages	22. Price
Unclassified	Unclassified	36	A03

NASA FORM 1626 OCT 86